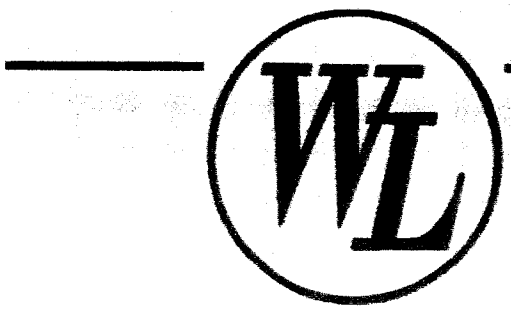

WHEELER LABORATORIES

122 Cutter Mill Road · Great Neck, N. Y.

A Subsidiary of Hazeltine Corporation

Report 1209

A MACROSCOPIC WAVEGUIDE MEDIUM FOR LASER SYSTEM COMPONENTS

By E. R. Schineller, D. W. Wilmot
and H. M. Heinemann

To National Aeronautics and
Space Administration
Contract Number NASw 888
1964 JUN 10 Job 466

myb
HWR
NAS

Summary

33168

Many applications in the fields of radar, communications, measurements, etc. have been proposed for coherent laser radiation. One approach to the design of systems for these applications is the utilization of conventional optical components; an alternative approach, which is being studied at Wheeler Laboratories, is the development of new optical components patterned after microwave devices. The initial step in the design of microwave-analagous components is the development of a single-mode optical waveguide large enough to permit component fabrication. Single-mode operation is required to prevent signal distortion due to modal dispersion.

A dielectric waveguide for this purpose has been studied and its feasibility has been demonstrated at optical frequencies. The waveguide dimensions are macroscopic in the sense that they are visible to the naked eye. It has been shown that a single-mode waveguide may be as large as 100 wavelengths with stringent but feasible tolerances on dielectric constant and surface quality. Single-mode and controlled multimode operation have been correlated with theory. In addition, a survey of materials and fabrication techniques has been made. One possible approach utilizes chemical diffusion techniques to obtain the needed control of dielectric constant.

Author

car

Contents

List of Figures

car

Contents (continued)

List of Figures — Page

Contents (continued)

List of Figures — Page

car

I. Introduction.

A laser system is generally composed of a laser oscillator and a collection of conventional optical components, such as lenses, prisms, beam splitters, etc. It has been recognized at Wheeler Laboratories that there is an alternate approach to the design of such systems. This approach is based on the realization that many of the proposed laser applications, particularly in the fields of communication and tracking, are analagous to currently existing microwave systems. This realization suggests the possibility of utilizing microwave-type components in the optical frequency range. Under the sponsorship of the National Aeronautics and Space Administration, Wheeler Laboratories is currently studying the feasibility of such an approach. This study involves (1) the development of a waveguide medium in which microwave-type components may be fabricated, (2) an evaluation of various component configurations, and (3) the fabrication of one or more microwave-type components to demonstrate the feasibility of this approach. This report covers the first phase of the study concerned with the development of the waveguide medium; a final report covering the development of components will be prepared upon completion of this study.

Microwave components are generally designed within a single-mode or controlled multimode medium. This approach has definite advantages over the unbounded character of conventional optical components. For instance, the power within a single-mode medium is constrained to propagate at only one set of angles determined by the waveguide dimensions and the frequency of the signal. Therefore, variations in the angle of incidence of the radiation at the input to the system affect only the excitation efficiency and not the character of the propagating mode. In an unbounded medium there is no such angular restriction and a variation in the angle of incidence at the system input many result in a variation of the properties of each individual component. An additional advantage of single-mode operation is that signal distortion caused by modal dispersion is prevented. In general, microwave components have well-defined phase characteristics. They are also angle insensitive and inherently more compact and stable than conventional optical components.

car

In order to duplicate the properties of microwave components the optical waveguide medium should operate in a single-mode or controlled multimode condition. It should also be macroscopic in size for ease of handling, feasibility of component fabrication and high-power capability. Waveguide operation at optical frequencies has been demonstrated in dielectric fibers (Refs. 13 and 16). However, in all previous single-mode experiments, the dielectric waveguide has had cross-sectional dimensions of a wavelength or less; while conventional dielectric fibers with diameters of the order of 100 wavelengths are known to support many propagating modes.

Dielectric waveguide consists of a core material of large dielectric constant embedded in a cladding material with a smaller dielectric constant. It may be shown that the maximum cross-sectional dimension for single-mode operation is inversely proportional to the square root of the difference between the dielectric constants of the core and cladding. This principle has been employed to obtain single-mode operation with cross-sectional dimensions exceeding 100 wavelengths. This waveguide exhibits an attenuation of several db/meter which makes it suitable for lengths of a few centimeters containing several components. The design and fabrication of such a waveguide is the topic of this Report.

The theoretical and experimental steps involved in the waveguide development are outlined herein. Section III presents the theory of optical dielectric waveguide and pertinent design data. Material considerations and fabrication techniques are summarized in Section IV. The experimental evaluation of the waveguide is outlined in Section V and results are reviewed in Section VI. The appendix contains an illustration of the theory of transverse resonance – a commonly used microwave technique which has proved invaluable in this study.

II. Symbols and Definitions.

x, y, z = rectangular coordinates. z is direction of propagation; x, y are transverse dimensions.

r = radial dimension of circular waveguide.

d = total width of core of slab waveguide.

D = diameter of core of circular waveguide.

Da = diameter of waveguide field.

W = total width of waveguide field.

W_i = width of focused incident field at half-amplitude points.

W_r = width of waveguide field at half-amplitude points.

A = area of waveguide field.

h = height of waveguide in y direction.

R = region of integration at waveguide aperture.

a = parameter indicative of width of gaussian curve.

P_r = total power received in waveguide.

P_i = total power incident on waveguide.

f_i = amplitude function of field incident on waveguide.

f_r = amplitude function of waveguide field.

ρ = power density of wave incident on waveguide.

η_a = aperture efficiency = ratio of power incident on aperture to that received.

θ = angle of plane wave in waveguide.

θ_c = critical angle for total internal reflection.

φ_o = angle of incident radiation in air.

φ = angle of incident radiation in waveguide medium.

k = dielectric constant.

k_1 = dielectric constant in core.

k_2 = dielectric constant in cladding.

Δk = $k_1 - k_2$.

ϵ_o = permittivity of free space.

λ = wavelength in free space.

λ_g = wavelength in waveguide.

K_o = free space propagation constant ($2\pi/\lambda$).

K_z = longitudinal propagation constant ($2\pi/\lambda_g$).

K_1 = transverse propagation constant in core.

K_2 = transverse propagation constant in cladding.

p = propagation parameter in core ($K_1 d/2$).

car

q = propagation parameter in cladding ($|K_2|d/2$).
Z = impedance.
Z_1 = transverse wave impedance in core.
Z_2 = transverse wave impedance in cladding.
Z_z = longitudinal wave impedance.
A_m = amplitude factor which determines absolute field strength.
n = integer.
m = mode number.
μ_{mn} = solutions of $J_n(\mu_{mn}) = 0$.
N = density of molecules.
α = polarizability.
e = charge on electron.
M = mass of electron.
f_s = oscillator strength.
ω_s = resonant frequency.
γ_s = damping term of quantum transition.

car

III. Optical Dielectric Waveguide Theory.

The theory of operation of dielectric waveguides is well-established and has received considerable treatment in the literature. Such waveguides have been treated for the microwave region in Refs. 11, 14, where the waveguide dimensions are generally of the order of a wavelength and the ratio of dielectric constants of the inner and outer regions is two or three to one. These microwave guides are usually constrained to a single mode of propagation.

Dielectric waveguides suitable for operation at optical frequencies have been treated in Refs. 5, 13, 16, 17. In some of these cases the difference in relative dielectric constants (Δk) between the inner (core) and outer (cladding) regions is large, and the waveguide size is many wavelengths, as is the case for many dielectric fibers employed in fiber optics applications. Therefore, these guides are highly multimode and the characteristics can generally be determined by a geometric optics analysis (Ref. 13). In other cases, the Δk has been reduced to about 0.01 by using a glass cladding with dielectric constant close to that of the glass core. However, even though the Δk is small, these waveguides still operate multimode unless the guide size is reduced to about one wavelength (Ref. 16).

The optical waveguide discussed in this report has dimensions large with respect to the wavelength, but operates with a very small Δk (0.0001). Under these conditions the guide can be constrained to operate in only a single mode or a few controlled low order modes, thus combining the advantages of large size with single mode propagation.

In the first part of this Section the properties of dielectric waveguide modes are discussed and a few of the structures capable of propagating such modes at optical frequencies are indicated. Then the conditions for obtaining single mode propagation with structures having large (macroscopic) dimensions are indicated. Various propagation characteristics of this "macroscopic" single mode guide are presented and finally the excitation and radiation properties of the guide are discussed.

In the more familiar case of metal waveguides, such as those used at microwave frequencies, the wave is guided along the structure by multiple reflections at the metal boundaries. For dielectric guides, the wave may also be guided by multiple reflections from the dielectric interfaces by the process of total internal reflection. The particular configuration of the guide may take on many forms; the primary requirement is that the dielectric constant of the inner medium (core) be greater than the outer medium (cladding), so that total internal reflection may occur. Two common configurations of dielectric waveguides are shown in Fig. 1. The slab configuration (Fig. 1(a)) is an unbounded structure on two sides and hence is limited to controlled-mode propagation in only one transverse direction. However it is very useful experimentally because of its simplicity, both of analysis and of construction. The dielectric rod waveguide shown in Fig. 1(b) is limited to controlled mode propagation in both transverse planes and hence can be true single mode.

A simple concept of propagation along these structures can be obtained by considering rays reflecting back and forth along the guide, as illustrated in Fig. 2, for the slab configuration. The propagating modes correspond to rays which are totally reflected at the dielectric interfaces and therefore travel down the guide without loss, as in Fig. 2(a). Only certain discrete angles of propagation are permitted, corresponding to angles which satisfy all the field conditions at the boundaries of the structure. The waveguide parameters can be chosen so that only one such angle will propagate; this is a single (fundamental) mode guide. In a single mode transmission medium, energy may propagate with only one stable field configuration. This means the field patterns in any cross-sectional plane of the transmission line are identical in shape. In guides capable of supporting a few modes, there are a few different field configurations which also may satisfy the conditions for propagation.

There is another class of modes called "leaky" modes which correspond to rays which are incident on the dielectric interfaces at an angle of incidence less than the critical angle and hence are not totally reflected. In this case, illustrated in Fig. 2(b), the energy traveling down the guide is strongly attenuated because power is lost at each reflection. The angles of propagation permitted in

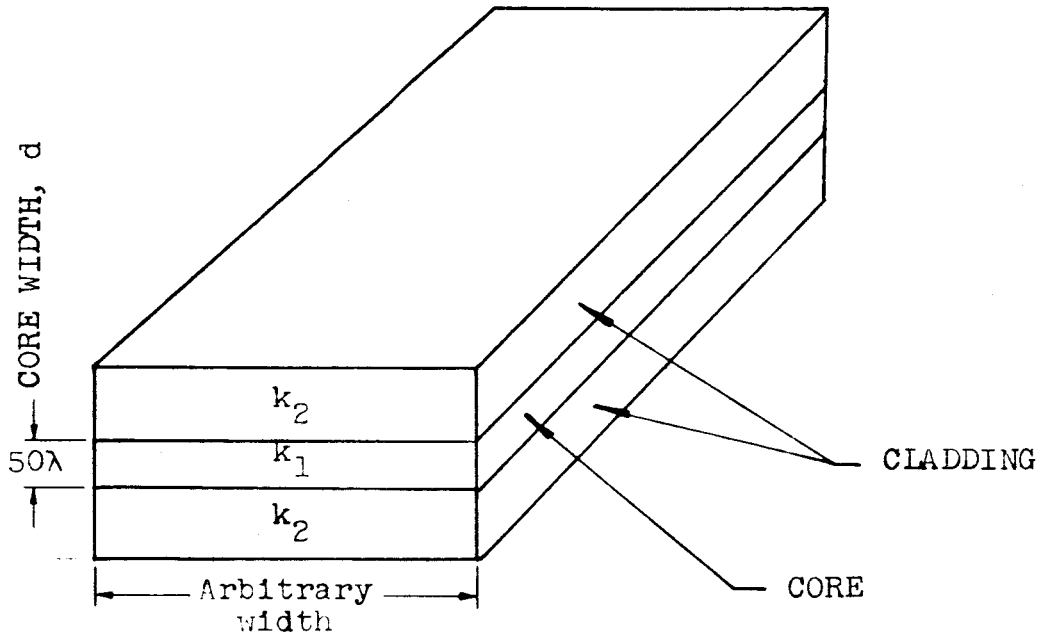

(a) Dielectric slab waveguide.

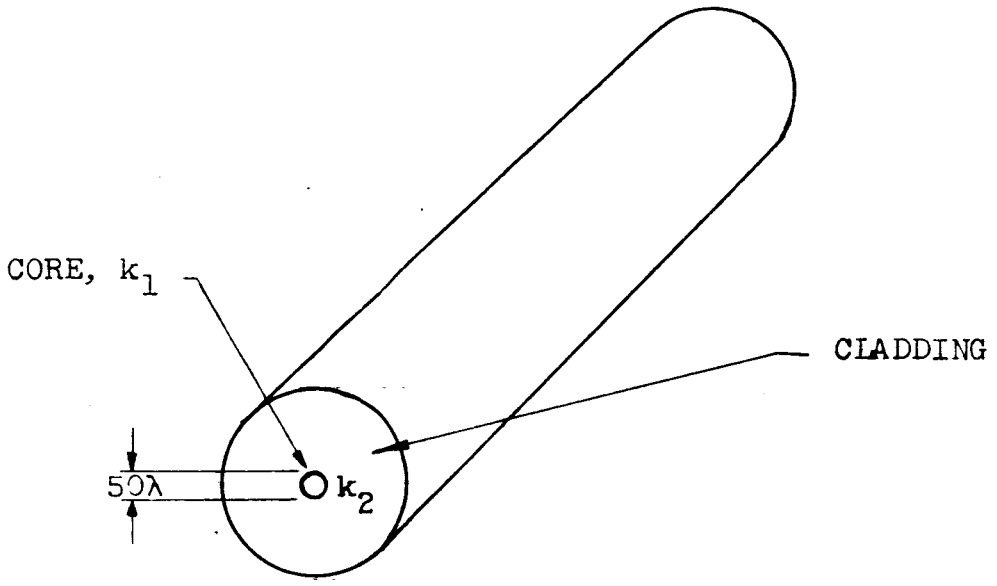

(b) Dielectric rod waveguide.

Fig 1 - Macroscopic dielectric waveguide.

bbs

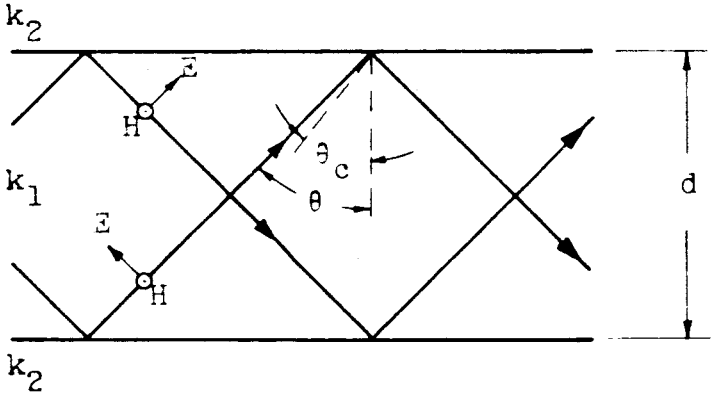

(a) Propagating TM mode.

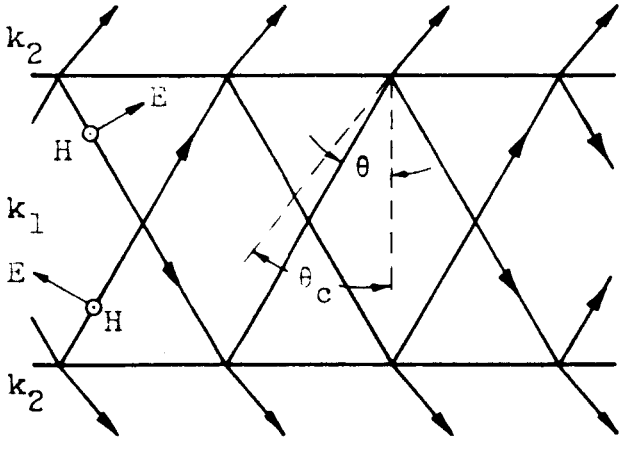

(b) "Leaky" TM mode (not propagating).

Fig. 2 - Propagation in a dielectric slab waveguide.

bbs

the waveguide are discrete for the leaky waves also; however, it is not possible to limit the number of leaky modes for a given size structure.

A more rigorous and complete analysis of propagation in dielectric waveguides is required to obtain the detailed propagation characteristics. These analyses have been presented in the literature in general terms using both field matching techniques (Ref. 5) and waveguide techniques (Ref. 14). In order to gain further insight into the characteristics of these waveguides, a complete analysis has been performed in the present study, using the transmission line approach known as "transverse resonance". The transverse resonance analysis (Ref. 6) seeks resonant conditions in the transverse plane as a criterion for propagation in the longitudinal direction. From this analysis, the propagation constants, field distributions, etc., can be determined. The basic details of the analysis are given in Appendix I, which presents a complete analysis for the slab configuration; the significant results are given in the remaining parts of this Section.

As shown in the Appendix, the properties of any dielectric waveguide can be determined from two pairs of characteristic equations. Each pair of equations corresponds to the transverse electric (TE) and transverse magnetic (TM) modes. The TM and TE modes are orthogonal, since they are linearly polarized in mutually perpendicular directions. In the special case of waveguides with very small differences in dielectric constants between the core and cladding, the propagation characteristics are degenerate and apply equally well to TE and TM modes, so that only one pair of equations need be specified. The two characteristic equations for the slab waveguide with small Δk are:

$$p \tan\left(p - \frac{m\pi}{2}\right) = q \qquad (1)$$

and

$$p^2 + q^2 = K_o^2 \frac{d^2}{4} (k_1 - k_2) \qquad (2)$$

where p and q are parameters related to the transverse propagation constants in the core and cladding regions respectively, K_o is the free space propagation constant $(2\pi/\lambda)$, d is the core width and k_1 and k_2 are the dielectric constants of the core and cladding respectively. These symbols are also defined in Section II. The conditions for waveguide propagation correspond to values of p and q which simultaneously satisfy the above equations. Since equation (1) is transcendental, the solutions are obtained by graphical techniques. The two equations are plotted on p vs. q coordinates in Appendix I; solutions of the two equations occur where the two curves intersect.

The condition for the waveguide to support propagation in a particular mode can therefore be readily determined from these characteristic curves. In order for a TM-m or TE-m mode to propagate, the following condition must be satisfied:

$$\frac{d}{\lambda}\sqrt{\Delta k} \geq \frac{m}{2}, \qquad (3)$$

where $m = 0, 1, 2, \ldots$ and $\Delta k = k_1 - k_2$. For the above condition, all modes of order m or lower will propagate. If $(d/\lambda)\sqrt{\Delta k}$ is less than $m/2$ the modes of order m and higher are leaky. This equation therefore defines a waveguide cutoff condition, where cutoff is defined as the transition point between propagating and leaky (or cutoff) modes. A convenient method of representing these relationships is by means of a mode chart (Ref. 19). This chart, shown in Fig. 3 has Δk plotted vs. d/λ. On these coordinates are drawn constant-m contours which graphically represent equation (3). These contours form the cutoff lines of the individual modes. A particular set of waveguide parameters (Δk and d/λ) define an operating point on the chart. For an operating point to the right of a given mode line m, all of the TM and TE modes of order m and lower will propagate. If the operating point is to the left of a given mode line m, the modes of order m or greater are leaky.

The number of propagating TM or TE modes in a given guide is one more than the mode number of the highest propagating mode, since $m = 0$ is the first mode. For the above condition there are actually $2(m + 1)$ propagating modes, since there are both TM and TE modes for each m. However, since these have identical propagation

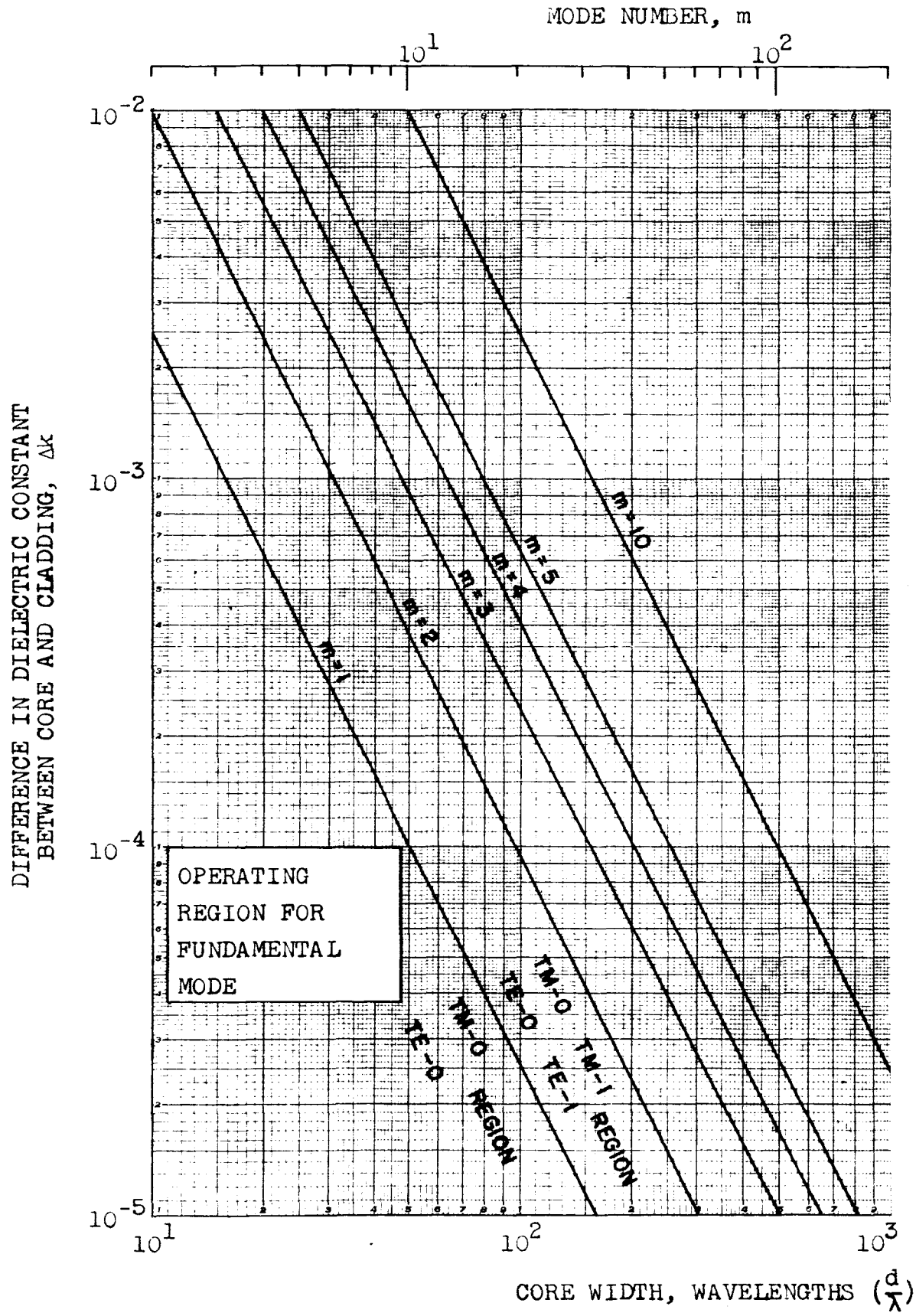

Fig. 3 - Mode chart for dielectric slab waveguide.

vmg

characteristics and since one or the other can be selected by choosing the appropriate polarization, the number of modes will be considered as m + 1 rather than 2(m +1). If the aperture field pattern in the waveguide were observed, the maximum number of lines (corresponding to peaks of the field pattern) which would be seen is also equal to m + 1. This fact is discussed further in connection with the experimental work presented in Section V.

In order to construct a single mode guide, the parameters must be chosen so that operation is restricted to the region to the left of the m = 1 line; this is the region marked TM-0, TE-0 on the chart. Such a guide is called single mode because although it supports both the TM-0 and TE-0 modes, these modes are degenerate for small Δk as mentioned previously. Also, since the modes are orthogonally polarized, one or the other can be selectively excited by choosing the appropriate polarization.

The characteristic equations and mode chart presented above have been derived for dielectric waveguide of the slab configuration. A similar set of equations can be derived for the case of a circular geometry. Although the details of the analysis differ, the general approach is identical to the slab configuration and so is not presented in this Report. The characteristics of circular waveguides have been treated in Refs. 5, 15, 17, and only the results are presented here.

A set of characteristic equations similar to equations (1) and (2) can be obtained for the circular guide and plotted on p vs. q coordinates as before. The corresponding mode cutoff relation for the special case of small Δk is

$$\frac{D}{\lambda}\sqrt{\Delta k} > \frac{\mu_{nm}}{\pi} \qquad (4)$$

The parameter, μ_{nm}, is a number obtained from the roots of the Bessel function (Ref. 17) whose value depends on the particular mode. (The mode notation follows that in this Reference.) A listing of the values of μ_{nm} for several low order modes is given on the mode chart for the circular dielectric waveguides shown in Fig. 4. This chart is analogous to the mode chart for slab waveguide (Fig. 3); as in the case of the slab configuration, the lowest order mode (HE-11) has no low frequency cutoff.

myb

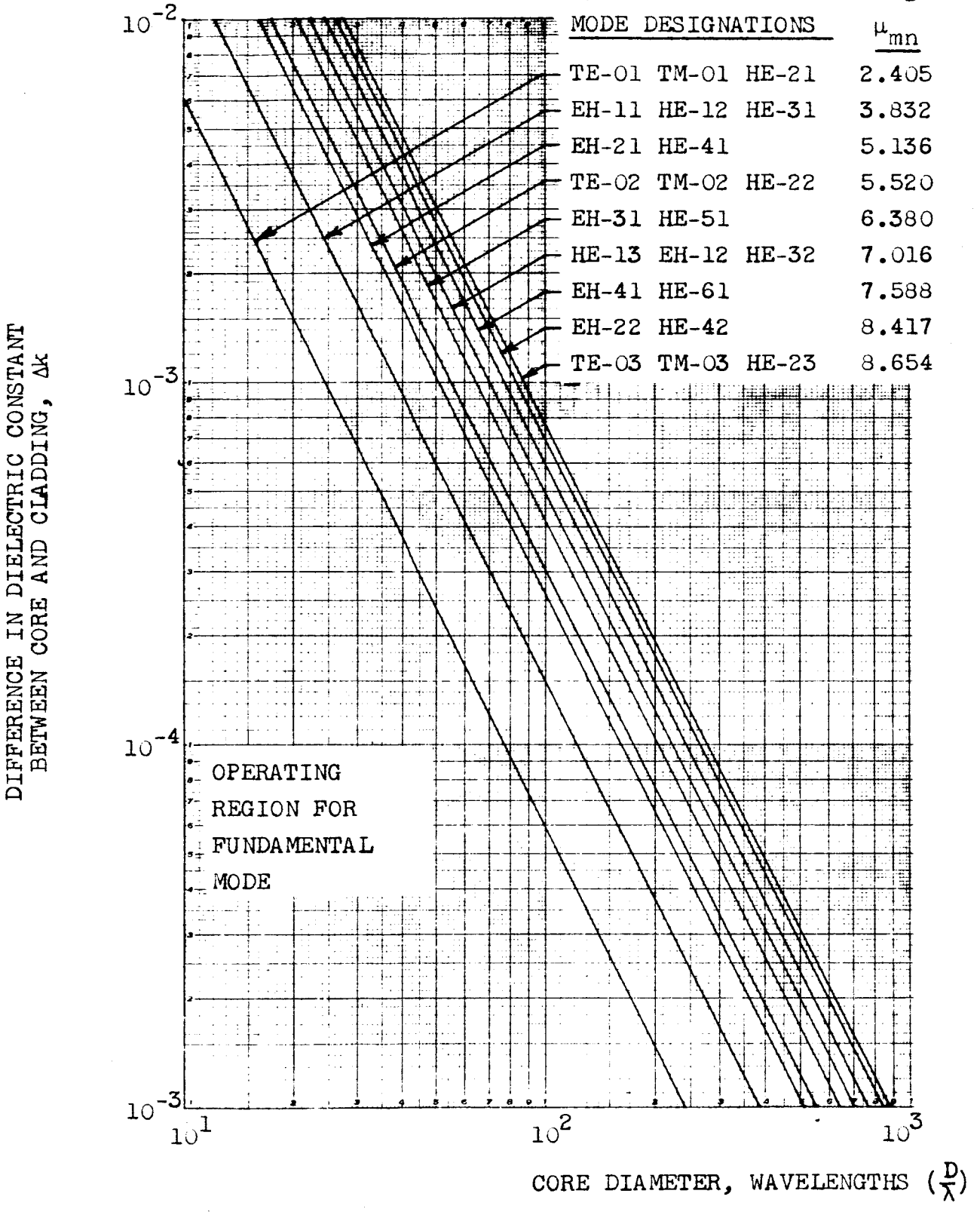

NOTE: Mode notation as in Ref. 17.

Fig. 4 - Mode chart for circular dielectric waveguide.

vmg

The distribution of the electric and magnetic fields within the waveguide, and the directions of the field lines has been determined for the slab guide, from the analysis in Appendix I.

The directions of the field lines of the TM-0 mode in slab waveguide are shown in Fig. 5(a); a sketch of the amplitude distribution of the transverse fields is shown in Fig. 5(b). Field patterns of the TM-1 mode are shown in Fig. 6. The patterns of the corresponding transverse electric (TE) modes may be obtained by interchanging the electric and magnetic field lines in these figures. It can be seen that the fields extend across the dielectric interface into the cladding region so that energy propagates in both the core and cladding regions. This result is not apparent from the simple analysis with reflecting rays mentioned earlier. Figs. 5 and 6 are intended to give a qualitative description of the fields, applicable to most operating conditions, rather than an accurate quantitative picture for a particular operating point.

A more accurate quantitative plot of the distribution of the transverse fields of the two lowest order modes of propagation is shown in Fig. 7, for a few different operating conditions. In all cases, the field distributions vary sinusoidally in the core region and exponentially in the cladding. The amplitude of the fields at the edge of the core depends on the operating conditions; the field strength at the edge increases as the mode becomes closer to cutoff. At the cutoff condition, the fields extend indefinitely into the cladding; consequently such a mode would require infinite energy to excite and is not useful. A typical operating point has been chosen as a condition where only the desired number of modes may propagate, and the highest mode is about 10 percent away from cutoff of the next higher mode on the p vs. q curves. The graphical determination of the operating points are shown in Appendix I and indicated on the plots in Fig. 7.

It can be seen from the field patterns of Fig. 5 for the TM-0 mode, that the electric field direction is normal to the waveguide surfaces at a plane through the center of the guide. Consequently a metal bisecting wall could be placed at this plane without affecting propagation. Similarly, for the TE-0 mode, a magnetic bisecting wall (open circuit) could be placed in the

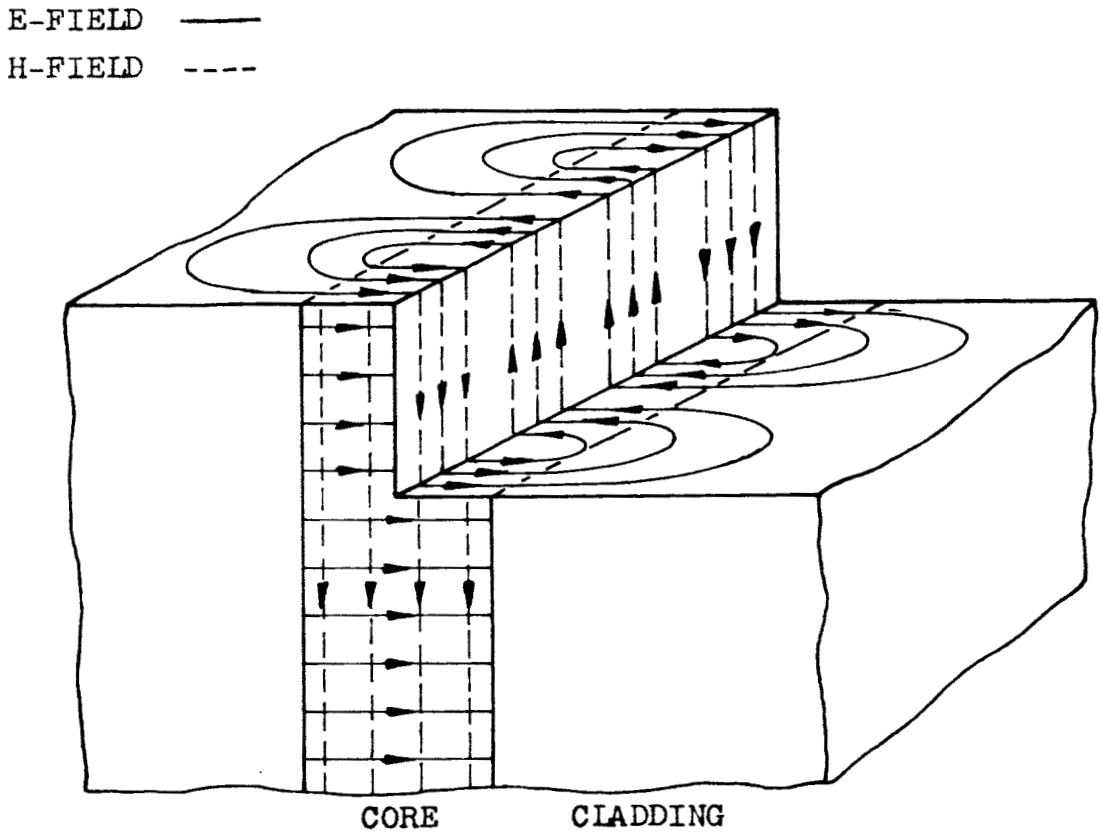

(a) Directions of field lines.

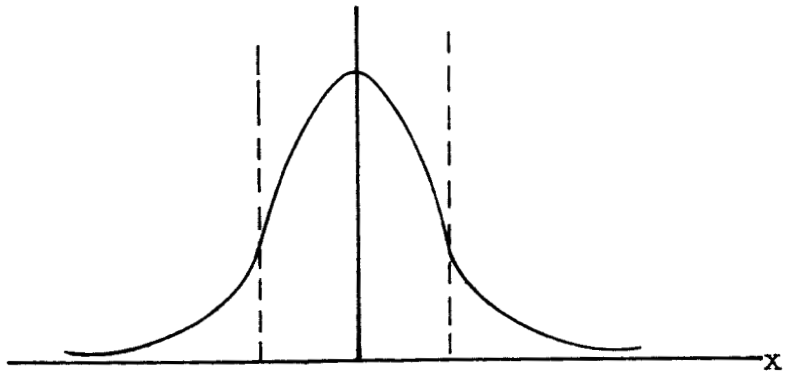

(b) Amplitude distribution of transverse field.

Fig. 5 - Field patterns of TM-0 mode in dielectric slab waveguide.

vmg

E-FIELD ——
H-FIELD ----

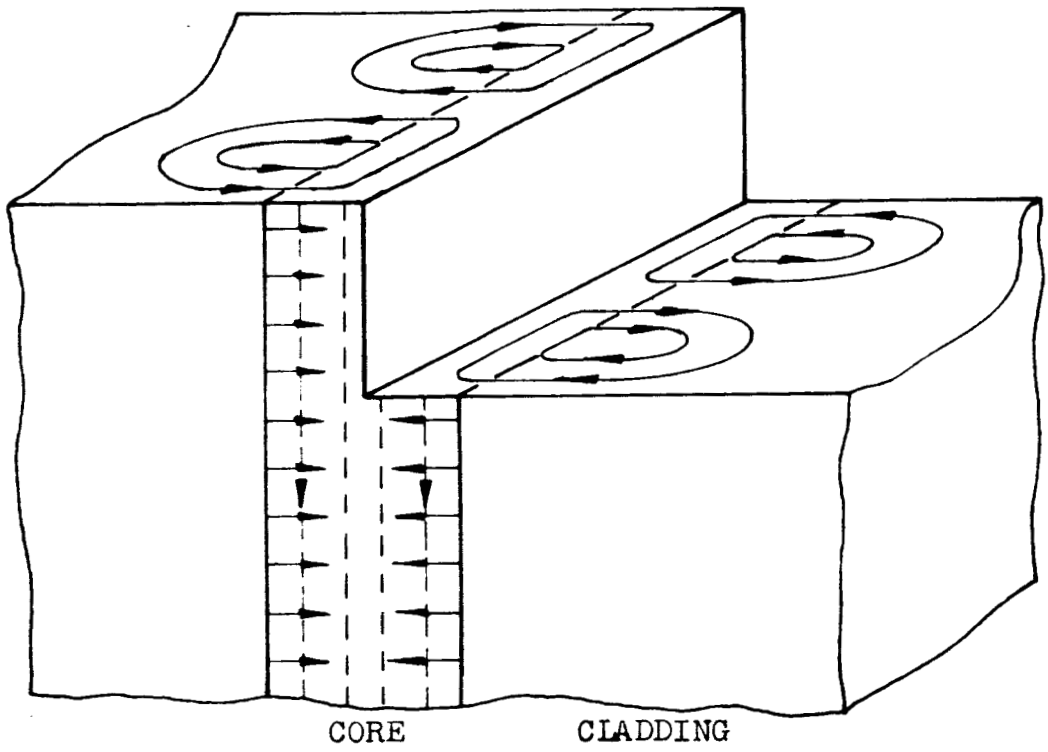

(a) Directions of field lines.

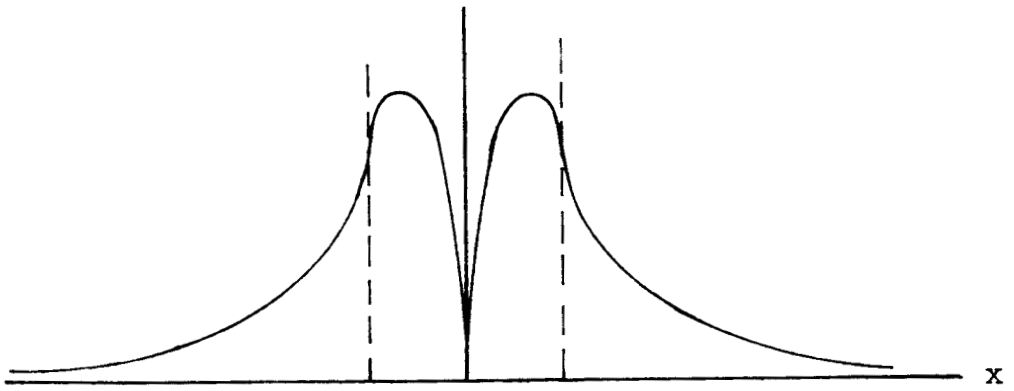

(b) Amplitude distribution of transverse fields.

Fig. 6 - Field patterns of TM-1 mode in dielectric slab waveguide.

vmg

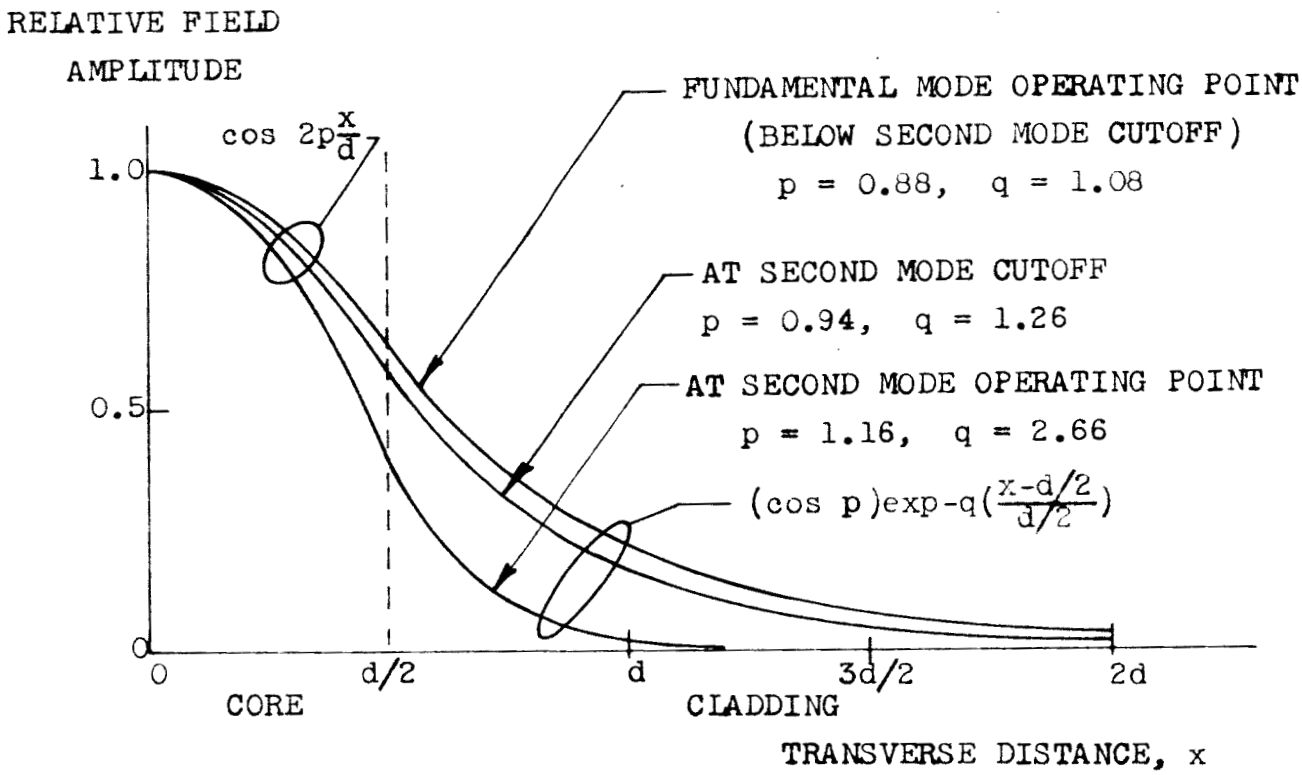

(a) Fundamental mode (TM-0 or TE-0).

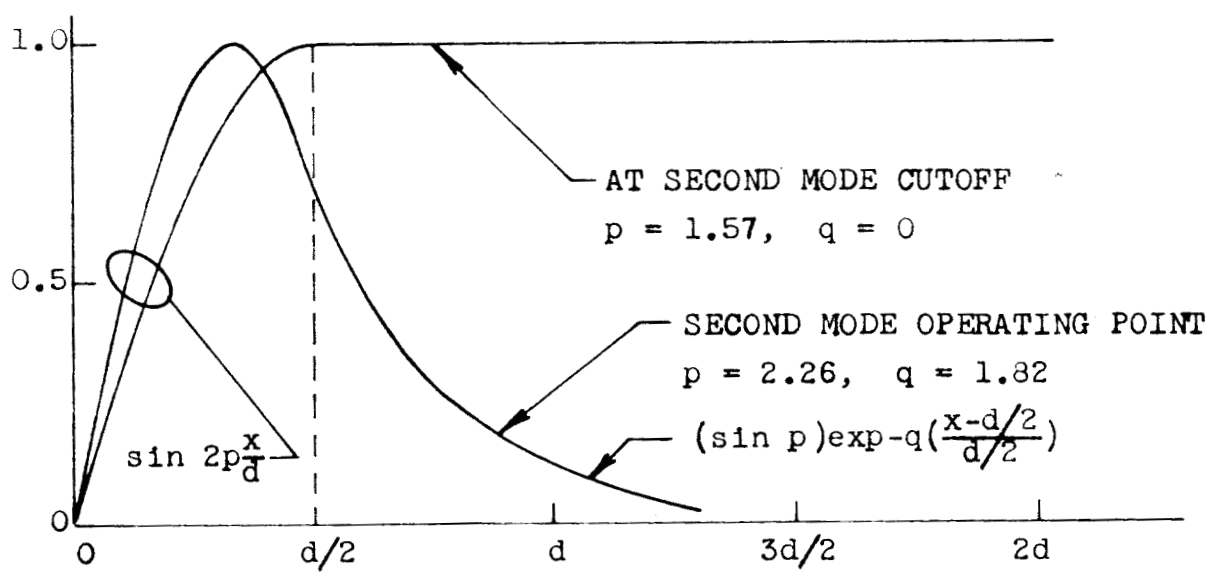

(b) Second mode (TM-1 or TE-1).

Fig. 7 - Transverse field distribution in dielectric slab.

vmg

center of the guide without affecting propagation. It is shown in the Appendix that a metal bisected waveguide propagates half of all the possible modes of a full width guide, and a magnetic bisected waveguide propagates the other half.

The field distribution in cylindrical dielectric waveguide can be calculated in a similar manner as for the slab (Ref. 5, 15). In this case, the fields in the core region are given by Bessel functions and in the cladding by Hankel functions. A sketch of the field lines of the fundamental (HE-11) mode in cylindrical guide is shown in Fig. 8(a). The field lines in the cladding have not been shown since this simplifies the picture, and as a practical matter, the field intensity is very low in the cladding for most operating conditions. It can be seen that the field lines in the core are parallel, and hence this mode is linearly polarized. Most of the higher order modes are not so simply polarized and hence not as adaptable to simple excitation techniques.

The distribution of the transverse fields in the cylindrical guide is shown in Fig. 8(b). This pattern is for the HE-11 mode, operating about 10% below the cutoff of the second mode.

Another important property of any waveguide is the variation of the propagation constant with frequency. This property, commonly called dispersion is calculated for the slab waveguide in Appendix I. A convenient method for presenting the dispersion properties of this type of waveguide is to plot normalized guide wavelength (λ/λ_g) vs. waveguide size normalized to free space wavelength (d/λ). A plot of the dispersion properties of the first and second modes is given in Fig. 9, for three different operating conditions. From these curves, the difference in guide wavelength between modes can be determined for any waveguide operating with a given Δk, guide size and frequency. It is interesting to note the limits of the guide wavelength for this type of waveguide. When operating far from cutoff, the guide wavelength approaches the wavelength of an unguided plane wave in the core region ($\lambda/\sqrt{k_1}$); when operating near cutoff, the guide wavelength approaches that of a plane wave in the cladding ($\lambda/\sqrt{k_2}$). Therefore for the waveguide under consideration, where the difference in dielectric constants between core and cladding is very small, the maximum dispersion between modes is also very small. The dispersion is

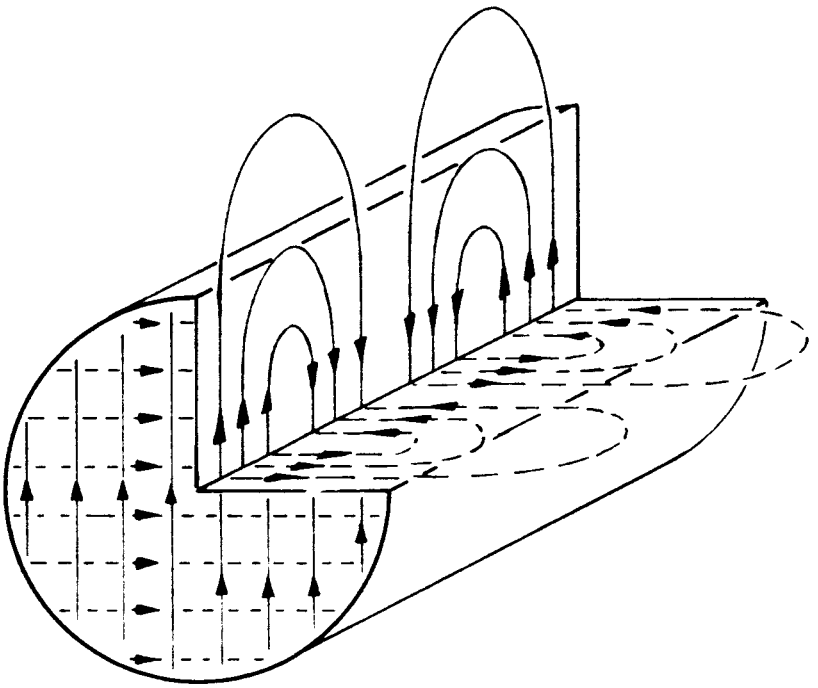

(a) Directions of field lines.

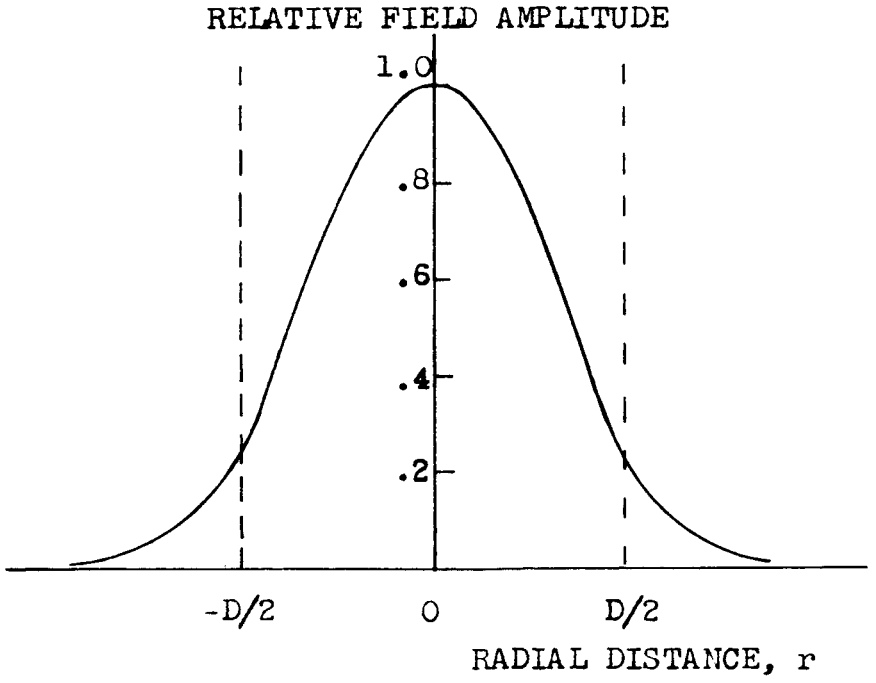

(b) Field amplitude (at fundamental mode operating point).

Fig. 8 - Field pattern of fundamental (HE-11) mode in cylindrical dielectric waveguide.

vmg

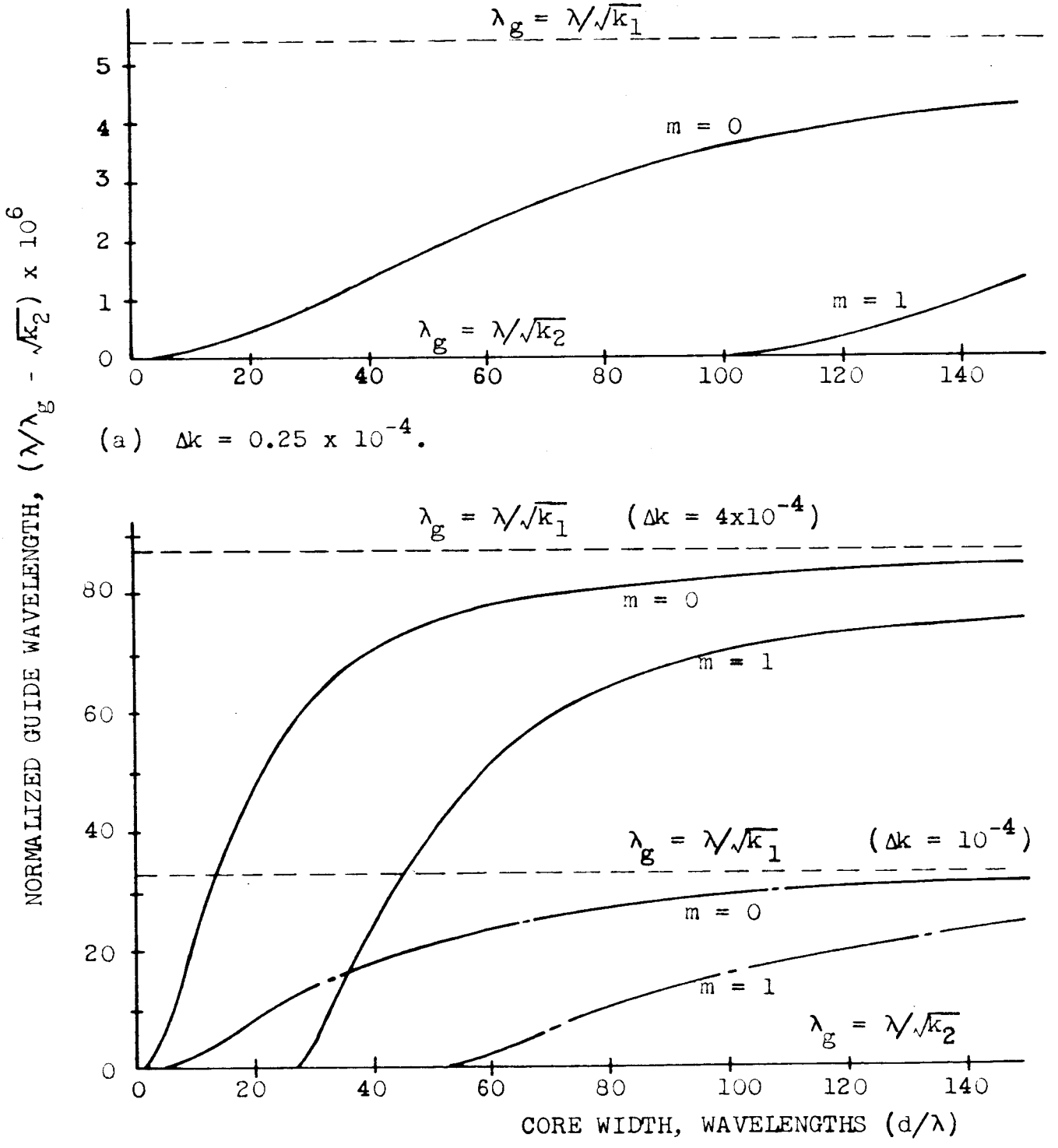

(a) $\Delta k = 0.25 \times 10^{-4}$.

(b) $\Delta k = 10^{-4}$; 4×10^{-4}.

Fig. 9 - Dispersion properties of dielectric slab waveguide.

vm

sufficiently large to permit construction of directional couplers which rely on dispersion between modes however, and in fact corresponds to coupling regions which are of convenient (macroscopic) size (about 1/2 inch).

All the previous calculations of propagation characteristics have assumed lossless media for both the dielectric materials and the metal bisecting walls (in the case of bisected waveguide). Under these conditions, there is zero attenuation for the propagating modes; the leaky modes are of course highly attenuated in the direction of propagation.

The effects of lossy propagation media on propagation have been investigated briefly. For a waveguide composed of dielectric materials only (core and cladding) the waveguide attenuation is very nearly equal to the attenuation of an unguided plane wave through the same medium. If the losses of the core and cladding regions differ, the resultant attenuation of the waveguide is equal to the sum of the unguided attenuation in each medium multiplied by the percentage of the total power in the respective region (Ref. 8). For normal operation, most of the power is concentrated in the core region and so if the losses of the two regions are of the same magnitude, the attenuation is determined almost entirely by the loss of the core medium. Data on typical values of loss for some of the materials being considered for waveguide construction are given in the next Section on materials and fabrication. The attenuation of the experimental waveguide presently being tested is about 3 db per meter.

The attenuation of a bisected waveguide configuration is caused by the loss of the dielectric medium and the bisecting wall. The loss caused by the dielectric medium is the same as for the ordinary waveguide discussed above. The loss caused by the bisecting wall is more complex because it may not only introduce attenuation, but can also affect the phase of the propagation constant.

A simple analysis of the affect of the lossy wall can be performed if it is assumed that the loss contributes only a small perturbation on the real propagation constant. The distribution of the fields in the bisected waveguide is then identical to the distribution in one half of a normal guide operating in the same mode. A simple method of calculating the loss then, is to consider the wave-

guide propagation as comprising two plane waves reflecting back and forth down the guide. The reflectance of the metal wall is less than 100% however, and so some power is absorbed at each reflection. The attenuation is therefore equal to the number of reflections per unit length multiplied by the power lost at each reflection. The reflectance, and hence the attenuation, is different for the two polarizations, and varies as a function of the angle of incidence. Therefore, the attenuation of the TM and TE sets of modes should be different. This simplified approach to the attenuation of the bisected guide predicts small attenuation for the TE modes and very large attenuation for the TM modes, at normal operating conditions.

However, a more detailed analysis of the propagation characteristics of a waveguide with a lossy-metal bisecting wall indicates that the propagation constant is affected strongly by the wall and so the simple analysis presented above is not adequate. The essential difference between the behavior of a perfectly conducting metal and a finite conducting metal occurs at angles of incidence near grazing (as is the case for the waveguide being considered). Here the lossy metal acts as a lossy dielectric, and consequently exhibits a Brewster angle effect, which changes the phase of the reflected wave, relative to that obtained with a perfect metal. The phase of the reflected wave is therefore the same for both polarizations, and as a result both TM and TE modes propagate in an almost identical manner. This phenomenon will be investigated further in this job; however, preliminary experimental results, presented in Section V, indicate that the propagation characteristics of both TM and TE modes are identical, as this theory predicts.

The problem of exciting the waveguide, treated here, concerns the coupling of optical power from some external source to the operating mode of the waveguide. The excitation characteristics of interest are the efficiency of excitation, the relative coupling for each mode of operation, and the dependence of coupling on angle of incidence. Usually, the external source is either far removed so that there is a uniform plane wave incident on the aperture, or the source is nearby so that there may be a sharply focused field on the aperture. The definition of efficiency depends on which case is being considered.

myb

For the case of plane waves incident on a waveguide aperture, it is convenient to first select an aperture area and then consider the amount of power incident on that area. This power is equal to the power density, in watts per unit area, multiplied by the area. To determine the coupling of the incident power to the aperture, an efficiency factor is defined, which is the ratio of the power coupled (or received) to the power incident within the aperture area. Therefore, the power received is (assuming impedance matching):

$$P_r = \rho A \eta_a$$

where ρ = incident power density (watts/unit area), A = aperture area and η_a = aperture efficiency. The aperture area is defined so as to include the fields developed by the mode under consideration as shown in Fig. 10. The aperture efficiency herein defined is called the "gain factor" in microwave antenna theory (Refs. 3, 18). The aperture efficiency shown in Fig. 10 for the slab waveguide is for a unit height, so the area of the aperture must be multiplied by the height of the guide under consideration.

The effect of angle of incidence on the coupling may also be computed from antenna pattern theory. In Fig. 11 are shown the normalized aperture distributions (waveguide field distribution) and the corresponding radiation patterns for several low order modes, which could be developed in rectangular metal waveguide (Refs. 3, 7). It should be noted that the particular distributions also apply to the dielectric slab waveguides when all the modes are "far from cutoff". This means that the guide will support additional higher modes besides those shown. It is observed that the higher modes have peak responses at angles far from the waveguide axis, and that these modes are therefore excited strongest by incident fields from off-axis directions. The relative excitation of each of these modes is illustrated in Fig. 12. In this case the aperture width is the core width (field amplitudes are very small in the cladding). The peak amplitudes shown are the aperture efficiencies, expressed as a voltage ratio ($\sqrt{\eta_a}$). A plane wave incident at the angle φ, as shown will excite the first, second and third modes in the voltage ratio 0.24, 0.74, 0.51 respectively.

myb

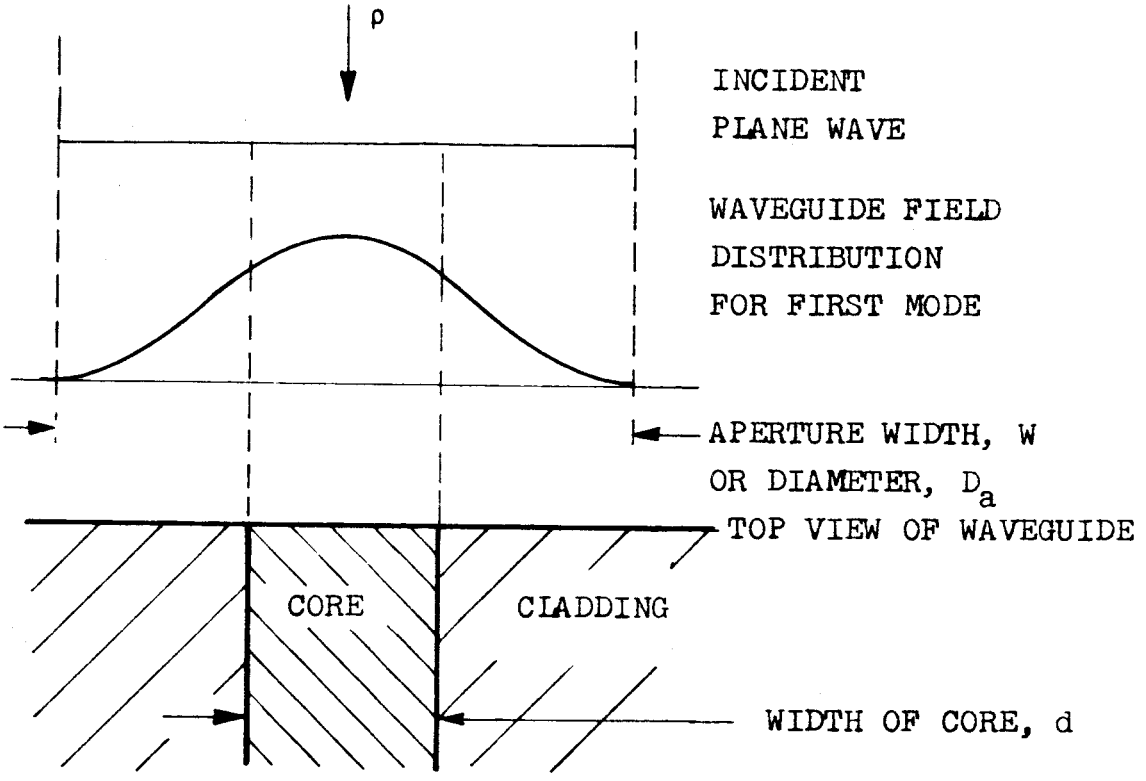

P_r = power coupled to waveguide mode
$= \rho A \eta_a$

where ρ = incident power density, watts/unit area

SLAB CONFIGURATION

$A = W \times h$
$\eta_a = 0.67$ (for cosine-squared field distribution)
h = height of waveguide under consideration

CIRCULAR CONFIGURATION

$A = \pi D_a^2/4$
$\eta_a = 0.56$ (cosine-squared)

Fig. 10 - Coupling to waveguide with plane wave.

vmg

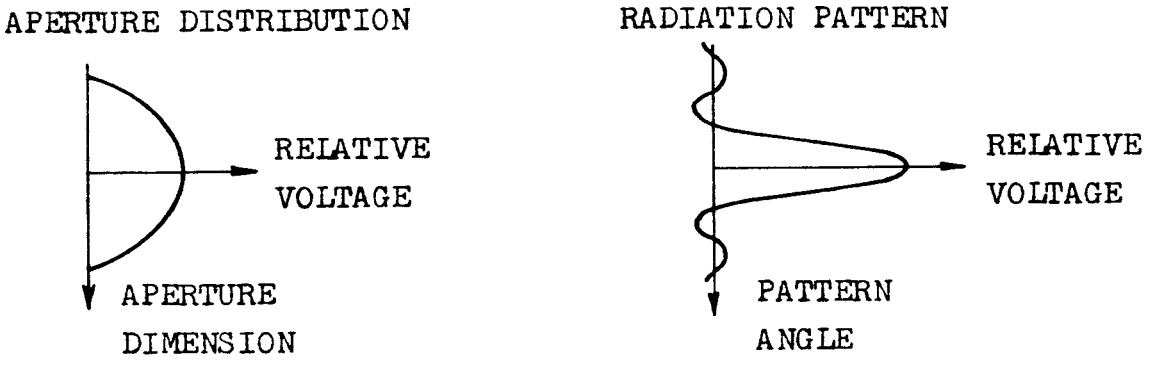

(a) TE-0, TM-0 modes.

(b) TE-1, TM-1 modes.

(c) TE-2, TM-2 modes.

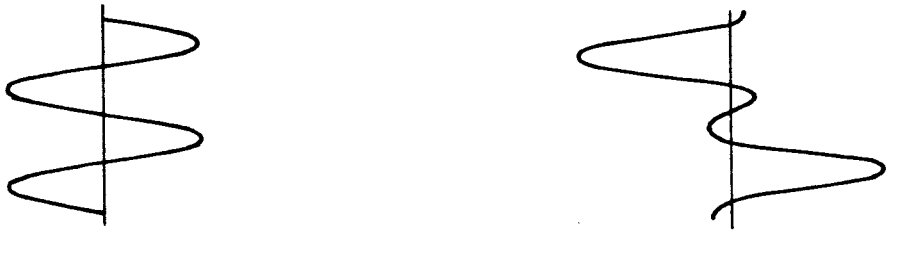

(d) TE-3, TM-3 modes.

(Note: all modes far from cutoff).

Fig. 11 - Waveguide field distribution with far-field radiation patterns.

vmg

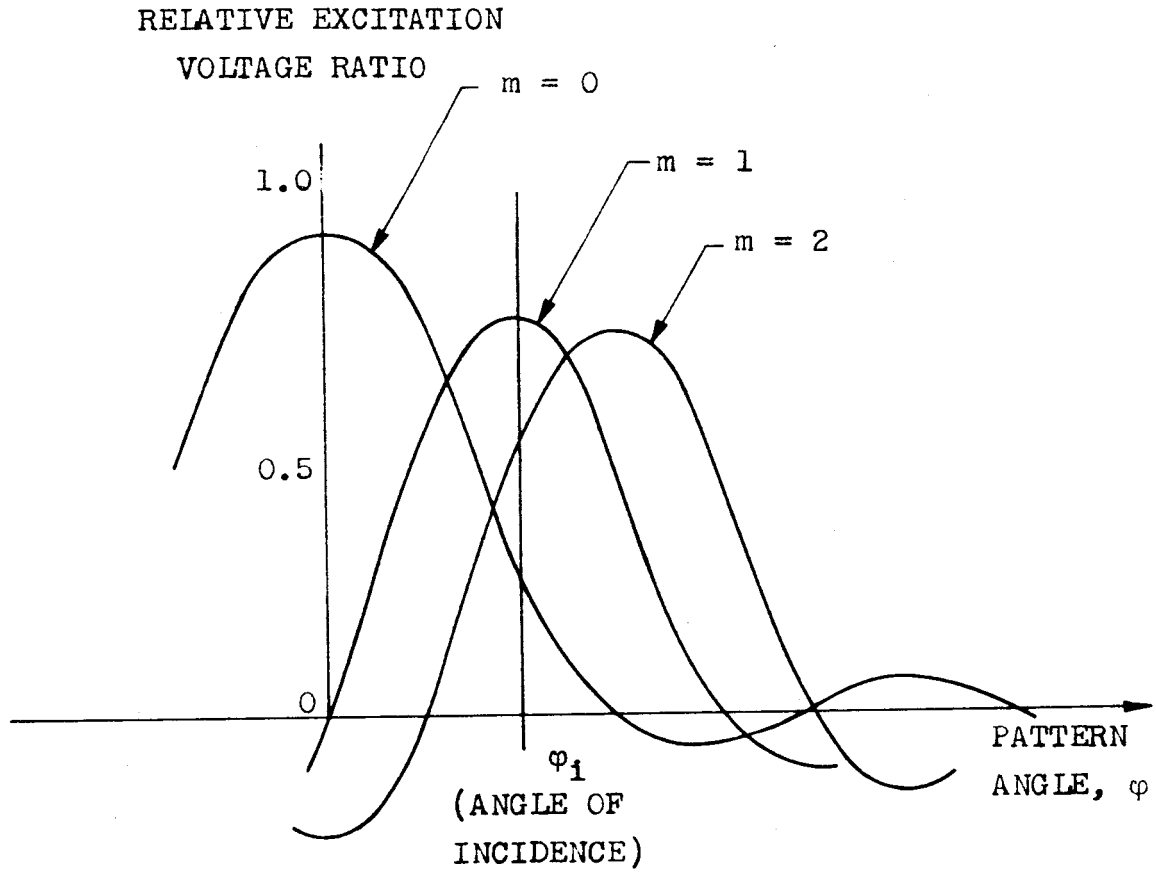

(a) radiation patterns.

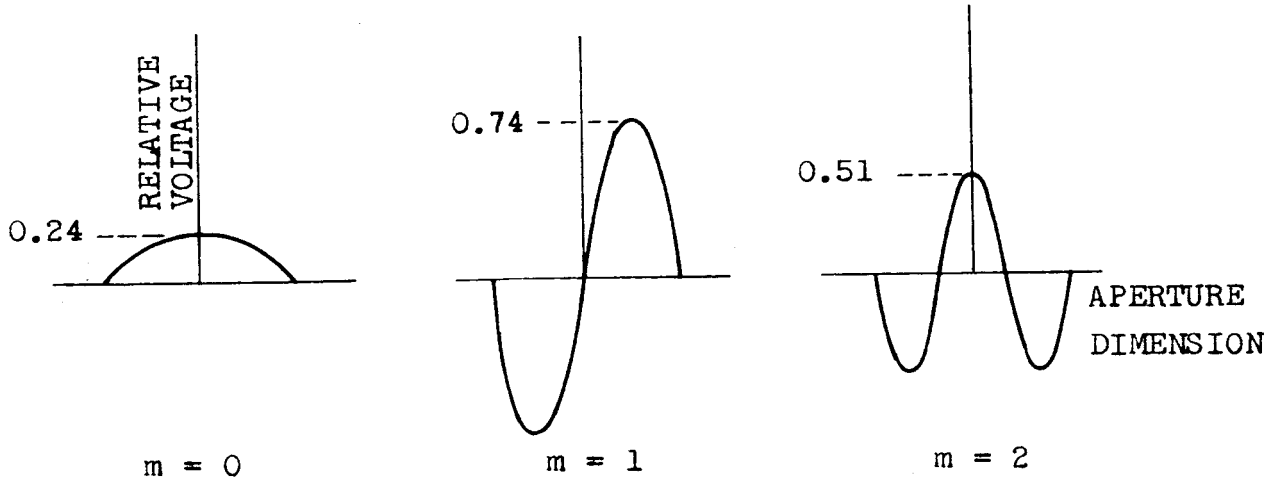

(b) aperture fields.

Fig. 12 - Relative mode excitation for a given angle of incidence.

vmg

For the case of external fields focused on the waveguide, not only is the width of the aperture significant, but also the width of the incident excitation. The coupling of power into the waveguide mode from the incident field depends on the similarity of the shapes of the incident and waveguide fields (Refs. 12, 20). When the fields have the same shapes, all the power of the incident field is coupled (assuming impedance matching). When the fields have different shapes, not all the power is coupled. The ratio of the power received to that incident is,

$$\frac{P_r}{P_i} = \frac{\left| \int_R f_i \, f_r \, dR \right|^2}{\int_R f_i^2 dR \int_R f_r^2 dR} \qquad (5)$$

where f_i and f_r are the distribution functions of the incident and waveguide fields and R is the aperture region. This formula may be evaluated in simple terms if the incident and waveguide fields are approximated by Gaussian shapes ($\exp - ax^2$); the results are summarized in Fig. 13. For the case of the slab waveguide, the coupled power applies to the coupling per unit height. If the incident field varies along the height dimension, each section along the height may be considered separately. For example, if the incident field is a circularly symmetric Gaussian and the widths of the incident and waveguide fields are the same, all the power may be coupled. However, the field in the waveguide in the height dimensions will then have the Gaussian shape. For circular fields and circular guides, the coupling applies to the total power.

For other angles of incidence and displacements of the fields, equation (5) may be applied, but evaluation is complex and is not carried out here. Qualitative considerations indicate that lateral displacement of the incident field will primarily affect the amplitude of the coupled signal, while changes of the angle will excite different higher modes, as in the case of plane waves incident.

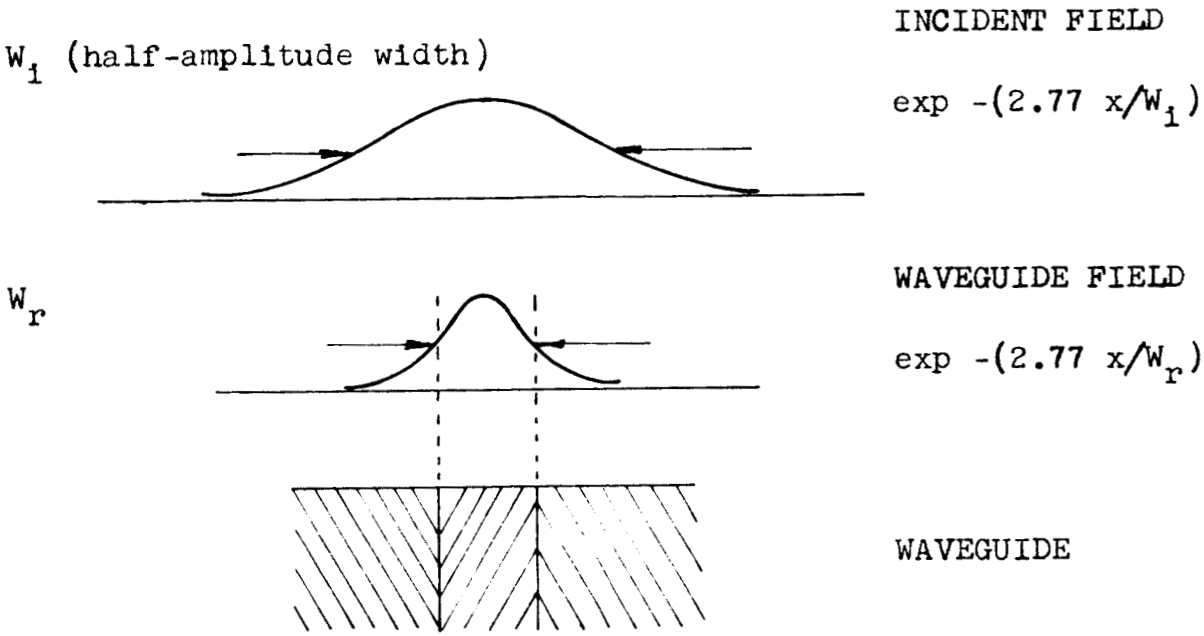

SLAB WAVEGUIDE

$$\frac{P_r}{P_i} = \text{ratio of power coupled per unit height}$$

$$= \frac{2}{\frac{W_i}{W_r} + \frac{W_r}{W_i}}$$

CIRCULAR WAVEGUIDE

$$\frac{P_r}{P_i} = \text{total power coupled}$$

$$= \left[\frac{2}{\frac{W_i}{W_r} + \frac{W_r}{W_i}}\right]^2$$

Fig. 13 - Coupling to waveguide with focused field.

vmg

IV. Waveguide Fabrication.

The ultimate objective of this optical waveguide study is the development of a medium in which practical optical components may be fabricated. In order to achieve this goal it is necessary to evaluate waveguide configurations and materials with respect to fabrication feasibility and practicality as well as propagation characteristics.

A. Configurations and Techniques.

Fabrication feasibility has been considered for two classes of waveguide models — (1) experimental models intended primarily for laboratory analysis of waveguide characteristics and (2) prototype models, with performance stable over a wide environmental range, to demonstrate practicality. The desired characteristics for these two classes are indicated in Table I.

Several experimental waveguide configurations are shown in Fig. 14 and their general characteristics are outlined in Table II. In all of these configurations either the waveguide core or cladding is a liquid. Such an arrangement eliminates the necessity for mating glass surfaces, reducing fabrication time and cost. Also, the temperature dependence of the dielectric constant of the liquid provides a convenient control of the difference in dielectric constant (Δk). However, this same temperature sensitivity will probably preclude its use as a prototype waveguide.

The box assembly shown in Fig. 15 has been used for most of the initial testing. The waveguide structure consists of two optically flat plates, 77 mm long, of Schlieren quality, borosilicate crown glass ($k = 2.2952$), suspended in chlorobenzene. The chlorobenzene in the gap between the plates serves as the waveguide core with the glass plates as the cladding. This construction permits easy adjustment of core size. The temperature of the waveguide is controlled to $.03^{\circ}C$ by a temperature-regulated, water-circulation system connected to the bottom of the box. Experimental data taken with this configuration is reported in Section V.

EXPERIMENTAL WAVEGUIDE MODELS	PROTOTYPE WAVEGUIDE MODELS
INTENDED USE: (1) Experimental verification of propagation constants and field configurations. (2) Medium for initial testing of component configurations. (3) Laboratory operation only.	INTENDED USE: (1) Demonstrate practicality of component construction. (2) Design stage preceding operational models. (3) Demonstrations external to the laboratory.
DESIRED CHARACTERISTICS: (1) Ease of parameter adjustment. (2) Tight control of all parameters to avoid ambiguity. (3) Adaptable to component feasibility studies.	DESIRED CHARACTERISTICS: (1) Fixed, stable parameters. (2) Loose tolerances to reduce fabrication costs. (3) Insensitivity to position. (4) Capability of operation over a reasonable temperature range. (5) Power capacity sufficient to handle conventional cw and pulsed lasers.

Table I. Desired characteristics of experimental and prototype waveguide models.

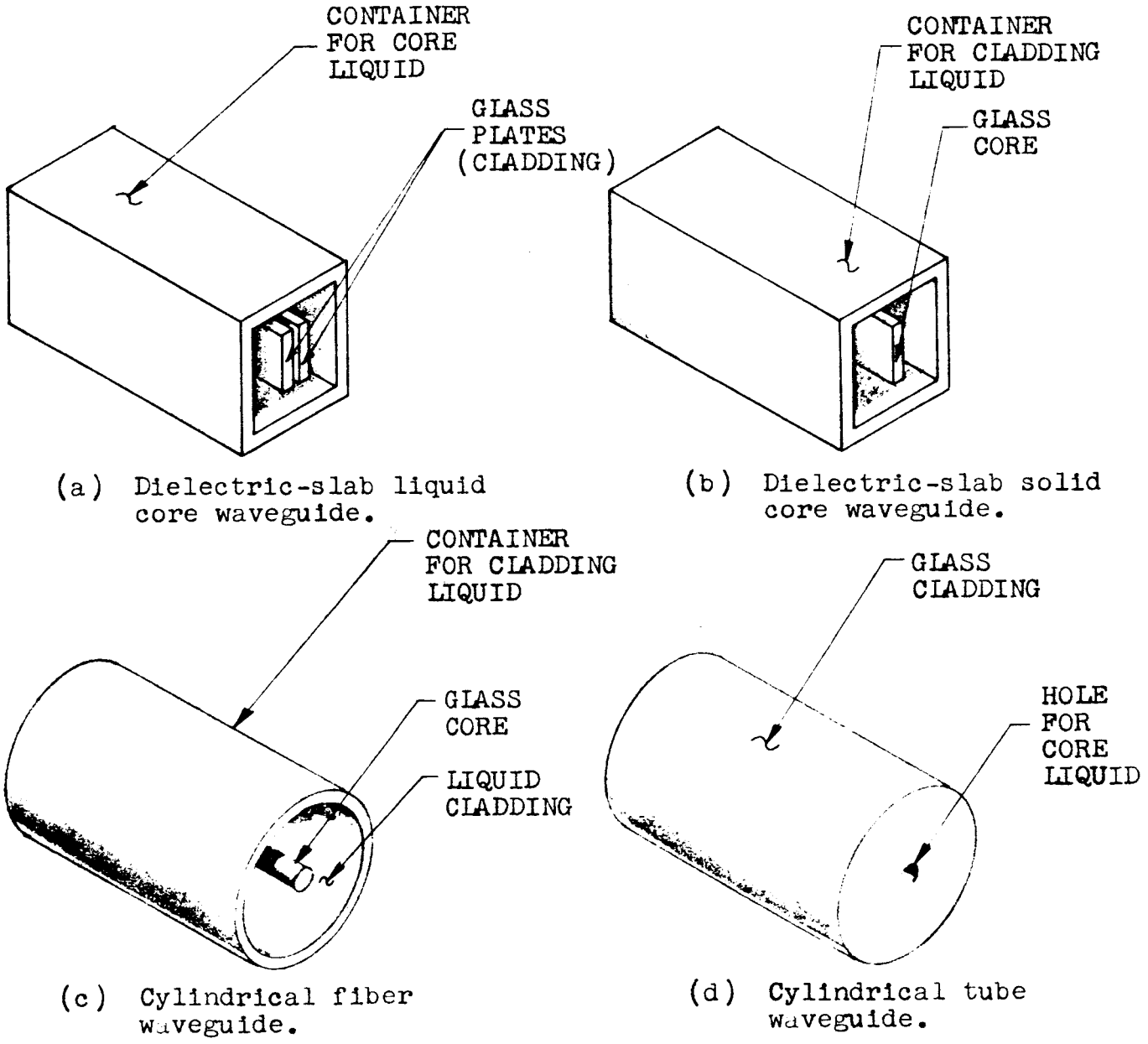

(a) Dielectric-slab liquid core waveguide.

(b) Dielectric-slab solid core waveguide.

(c) Cylindrical fiber waveguide.

(d) Cylindrical tube waveguide.

Fig. 14 - Sketches of experimental waveguide models.

vmg

WAVEGUIDE TYPE	CHARACTERISTICS
Dielectric-slab liquid core [Fig. 14(a)]	(1) Adjustable thickness. (2) Δk can be adjusted by temperature control. (3) Adaptable to component studies. (4) Easily modified to short circuit bisected configuration. (5) Inherently homogeneous liquid core. (6) Simple fabrication.
Dielectric-slab glass core [Fig. 14(b)]	(1) Δk can be adjusted by temperature control. (2) Adaptable to component studies. (3) Easily modified to short circuit bisected configuration. (4) Permits evaluation of effect of inhomogeneities in typical glass core. (5) Fabrication from available drawn sheets.
Cylindrical fiber [Fig. 14(c)]	(1) Δk can be adjusted by temperature control. (2) Single-mode in both cross-sectional dimensions. (3) Fabrication from available drawn glass or quartz fibers.
Cylindrical tube [Fig. 14(d)]	(1) Δk can be adjusted by temperature control. (2) Single-mode in both cross-sectional dimensions. (3) Fabrication from available glass capillary tubes or drawn quartz tubes. (4) Liquid may be sealed in tube, removing necessity for external container.

Table II. General characteristics of various experimental waveguide models.

vmg

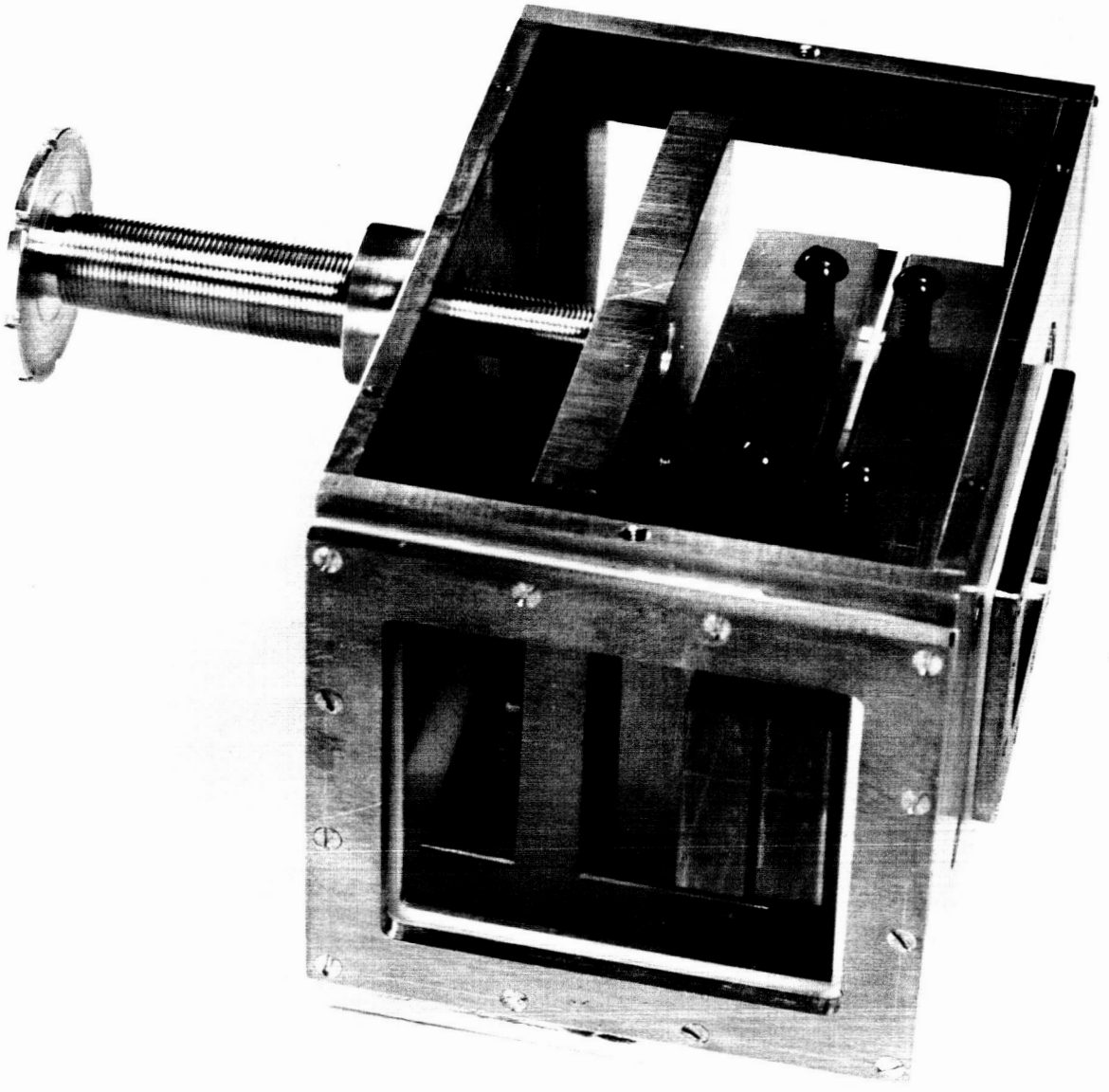

Fig. 15 - First experimental model of macroscopic optical waveguide.

vmg

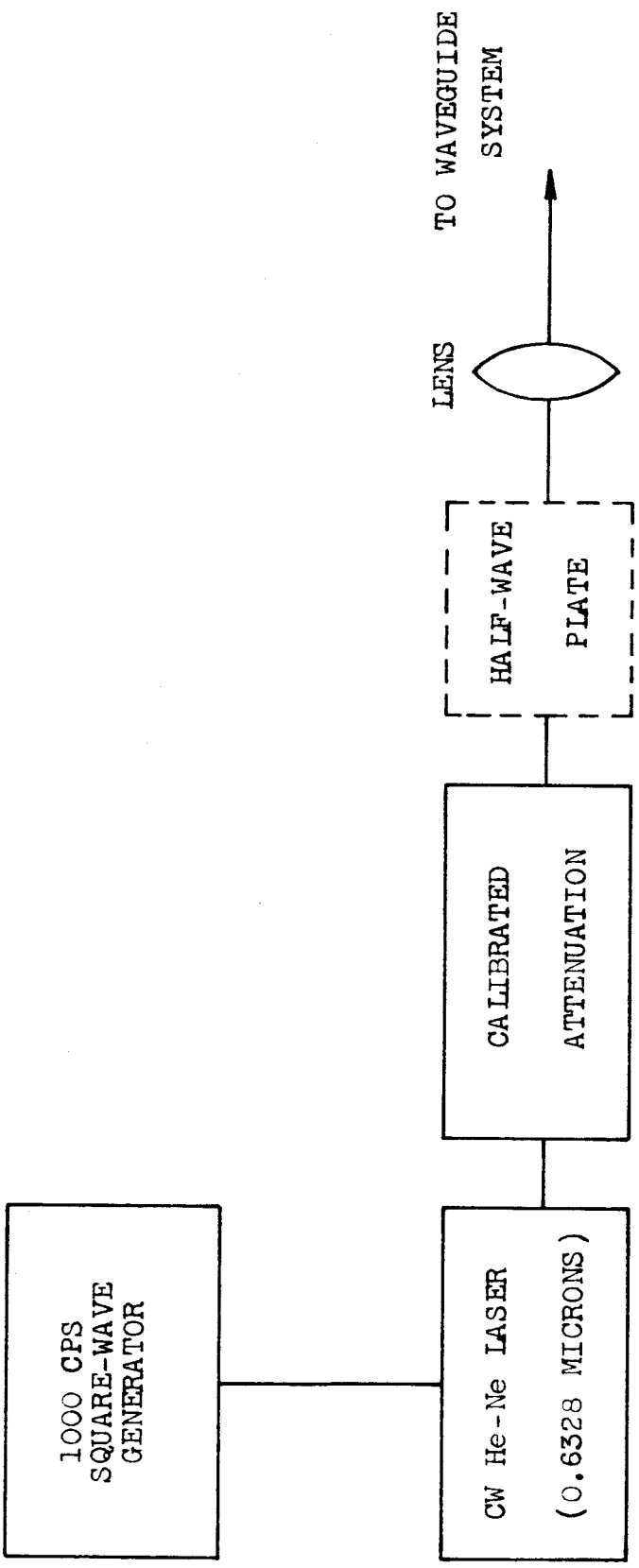

Fig. 24 - Block diagram of source system.

vmg

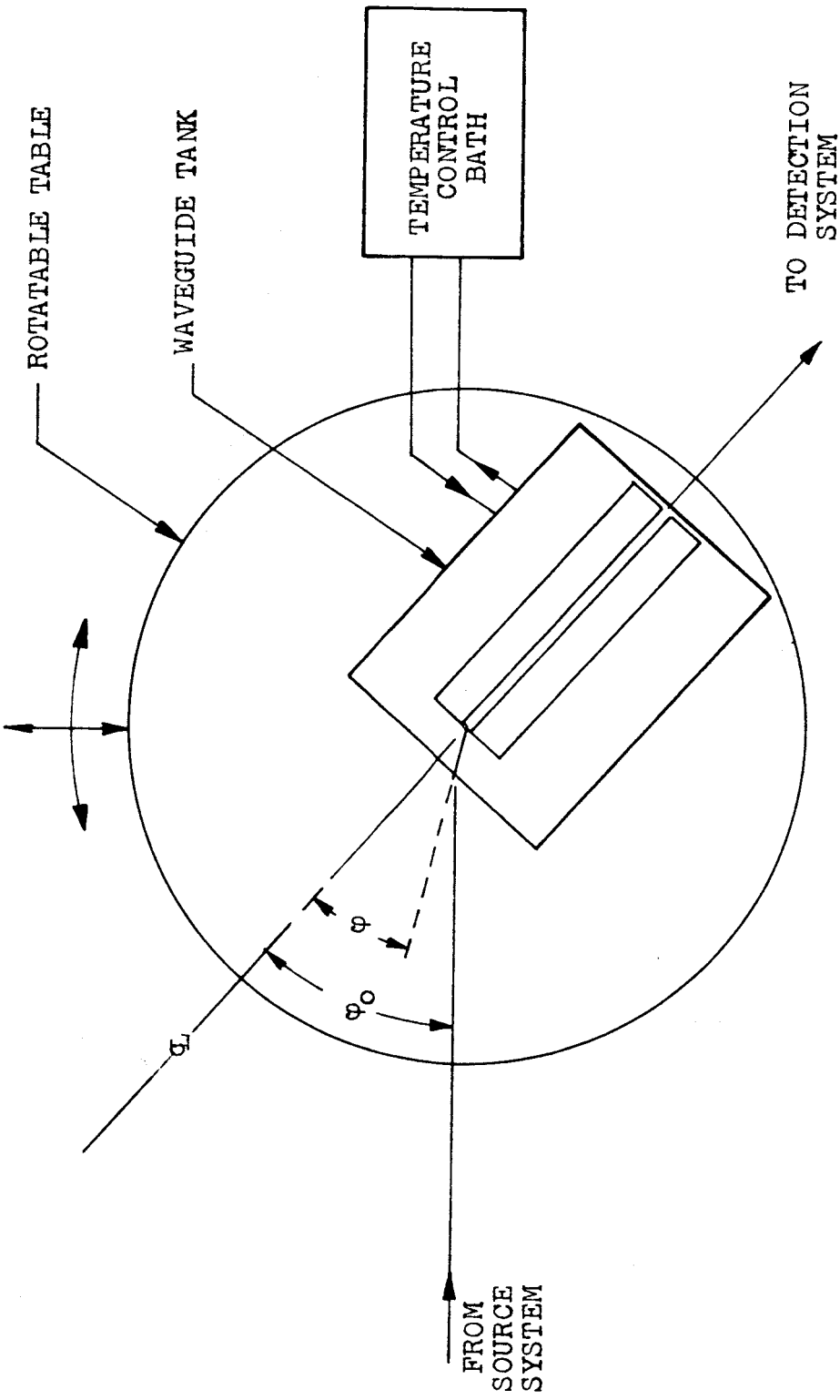

Fig. 25 - Block diagram of waveguide system.

waveguide relative to the incident laser beam. The temperature-regulation system is necessary to control the dielectric constant of the liquid in the waveguide, and therefore the difference in dielectric constant between the core and the cladding, as discussed in Section IV, Part B. The temperature of the waveguide may be controlled to $\pm 0.03^{\circ}$ C, and, therefore, the difference in dielectric constant is controlled to ± 0.00005. The waveguide tank is mounted on a table and may be rotated in the horizontal plane, in order to vary the angle of incidence of the laser beam (excitation angle). The table may also be moved transverse to the incident laser beam, in order to sample different portions of the beam.

The detection system, illustrated in Fig. 26, comprises a 1P22 photomultiplier tube and power supply, and either a tuned amplifier or a chart recorder, both of which respond to the 1000 cps modulation frequency of the laser. Both the recorder and amplifier are calibrated in decibels. A small rectangular aperture is placed in front of the photomultiplier to provide the requisite spatial resolution. In order to measure the aperture distribution of the waveguide, a 100X microscope is focused on the output aperture, and the pattern observed with the microscope is measured. The microscope is not employed when measuring the far-field (radiation) pattern of the waveguide. In addition to the above apparatus for pattern measurements, provision has been made for photographically recording the waveguide output.

The tests of the three waveguide configurations are described separately below.

1. Liquid-Core, Solid-Cladding Dielectric-Slab Waveguide.

For this waveguide configuration tests were made both of mode excitation and of aperture field distribution. The three parameters which could be adjusted are the difference in dielectric constant between the core and the cladding, the waveguide width, and the excitation angle of the waveguide. The width was adjusted to 35.7 microns (57λ) and then held constant throughout the test for the mode excitation study. The first step in the measurement was to increase the temperature until the waveguide became dark; at this

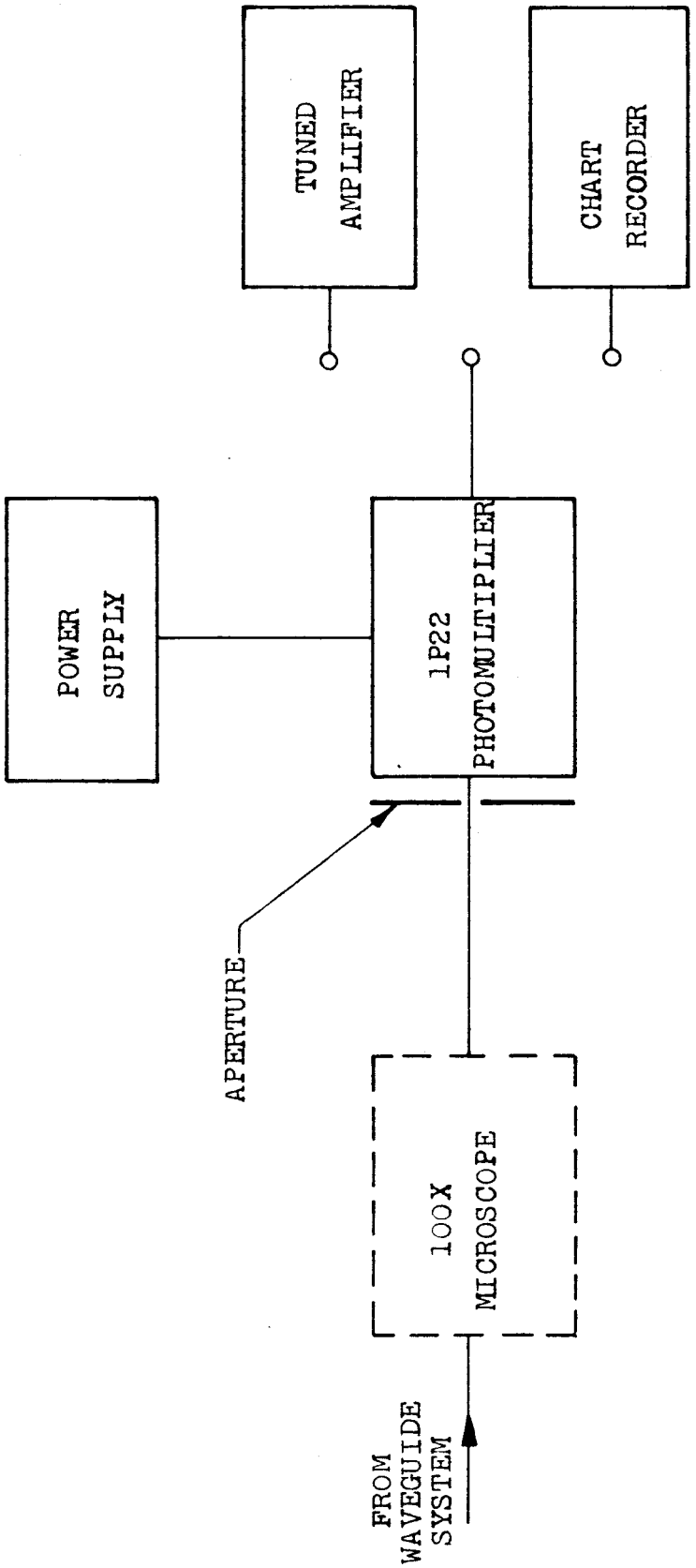

Fig. 26 - Block diagram of detection system.

For prototype waveguides several fabrication techniques have been considered. The general objective has been to obtain a waveguide fabricated entirely from solid materials. This objective is complicated by the small difference (10^{-4}) required between the dielectric constants of the core and cladding materials. Among the possible techniques are:

(1) Vacuum depositing of a dielectric cladding on a thin glass core. The dielectric constant of the cladding may be accurately controlled relative to the core by depositing a precise mixture of several dielectrics simultaneously.

(2) Diffusion of an impurity into the core material. The core and cladding would be fabricated from the same material and the diffused impurity would raise the dielectric constant of the core to the required value.

(3) Heavy doping of the cladding and controlled removal of the dopant to obtain the required dielectric constant for the cladding. In this case the core would be a pure material and the cladding material would be chosen so that its dielectric constant before doping was below that of the core. The adjustment of the dielectric constant could be made after the waveguide was assembled by immersing it in a chemical which removes the dopant in the cladding. Waveguide characteristics could be monitored during this process and the waveguide removed from the chemical when the desired Δk is obtained.

(4) Modification of the physical properties of a single glass slab to establish a k-gradient across it. The modal characteristics of this waveguide will differ somewhat from those discussed in Section III, but the important properties will be similar. Among the possible techniques for obtaining a k-gradient are: heat treating to change structure, diffusion of impurities into the slab, chemical reactions, nuclear processing, etc.

While the present experimental, partially liquid, models are suitable for waveguide studies and the evaluation of component

designs, the ultimate usefulness of macroscopic waveguide is its application to operational systems. Therefore, the fabrication of a prototype waveguide, consisting entirely of solid materials is of paramount importance.

B. Materials.

The fabrication of any optical waveguide involves a choice of materials which must be based on the effect of the material properties on waveguide propagation. A brief summary of pertinent material properties is presented in this subsection.

The properties of most interest are dielectric constant and dielectric loss. In addition, since metals may be used for waveguide bisections, metallic loss is also of interest. However, relatively high losses may be tolerated because the waveguide is to be used primarily for component fabrication, as opposed to long-run power-transfer applications. For instance an attenuation of 10 db/meter results in a loss of only 0.1 db for a one centimeter long component. On the other hand the tolerance on the homogeniety of the dielectric constant is quite critical. The required difference in dielectric constant between the core and cladding materials is of the order of .0001 for single-mode dimensions of a hundred wavelengths. Therefore, it is estimated that the dielectric constant throughout the core should not deviate by more than .00001 from its design value. The dielectric constant of the cladding must meet similar specifications in the region of the interface. However, this tolerance on the cladding becomes less critical at distances of one or two core thicknesses from the interface.

Dielectric losses arise from both absorption and scattering phenomena. In solid dielectrics scattering may be caused by large discontinuities such as air bubbles or scratches. These losses may be reduced to a negligible value by specifying optical quality, precision-annealed glass with a high quality surface finish.

Molecular scattering, which occurs in both liquids and solids, also contributes to dielectric loss (Ref. 10). This effect is directly proportional to the fourth power of frequency. Therefore,

this type of scattering, which is commonly neglected at microwave frequencies, must be evaluated at optical frequencies. For typical solid materials molecular scattering contributes about 1 db/meter to the attenuation at 1 micron.

Absorption is another important loss factor at optical frequencies. From an engineering point of view optical absorption need only be considered as a mechanism which reduces the intensity of the radiation in an exponential manner. The mechanism of absorption is related to the atomic structure of the material and is discussed in standard optical textbooks (Ref. 9).

Total loss is the important parameter for dielectric waveguide materials and this quantity may be easily measured. Therefore, detailed computations of dielectric absorption and scattering are not necessarily needed for the evaluation of dielectric materials. Empirical values for the total attenuation of glass and various liquids appear in the literature (Ref. 1). The total attenuation of transparent glass is generally given as less than 10 db/meter in the visible region. The attenuation of benzene and carbon disulfide have both been measured at WL to be about 3 db/meter at 0.6328 microns. As indicated previously, this magnitude of attenuation is considered acceptable for waveguide applications.

Metallic losses are significant because of their effect on reflection. In the short-circuit bisected waveguides a reflectance of 100% is desired. The degradation of waveguide performance with decreasing reflectance is indicated in Section III. The approximate reflectance of silver and aluminum are plotted in Fig. 16 as a function of frequency. This property is also a function of the angle of incidence. Fig. 16 is plotted for normal incidence; whereas, the reflectance at grazing incidence approaches 100% for both metals. In general, reflectance improves at the lower frequencies. Although silver has a higher reflectance, aluminum is usually preferred for its corrosion resistance.

Since the precise control of the dielectric constant of the waveguide materials has a critical effect on waveguide characteristics, it is necessary to understand the functional variation of this parameter. The dielectric constant of a pure material is related to molecular density and molecular polarizability by the

vmg formula;

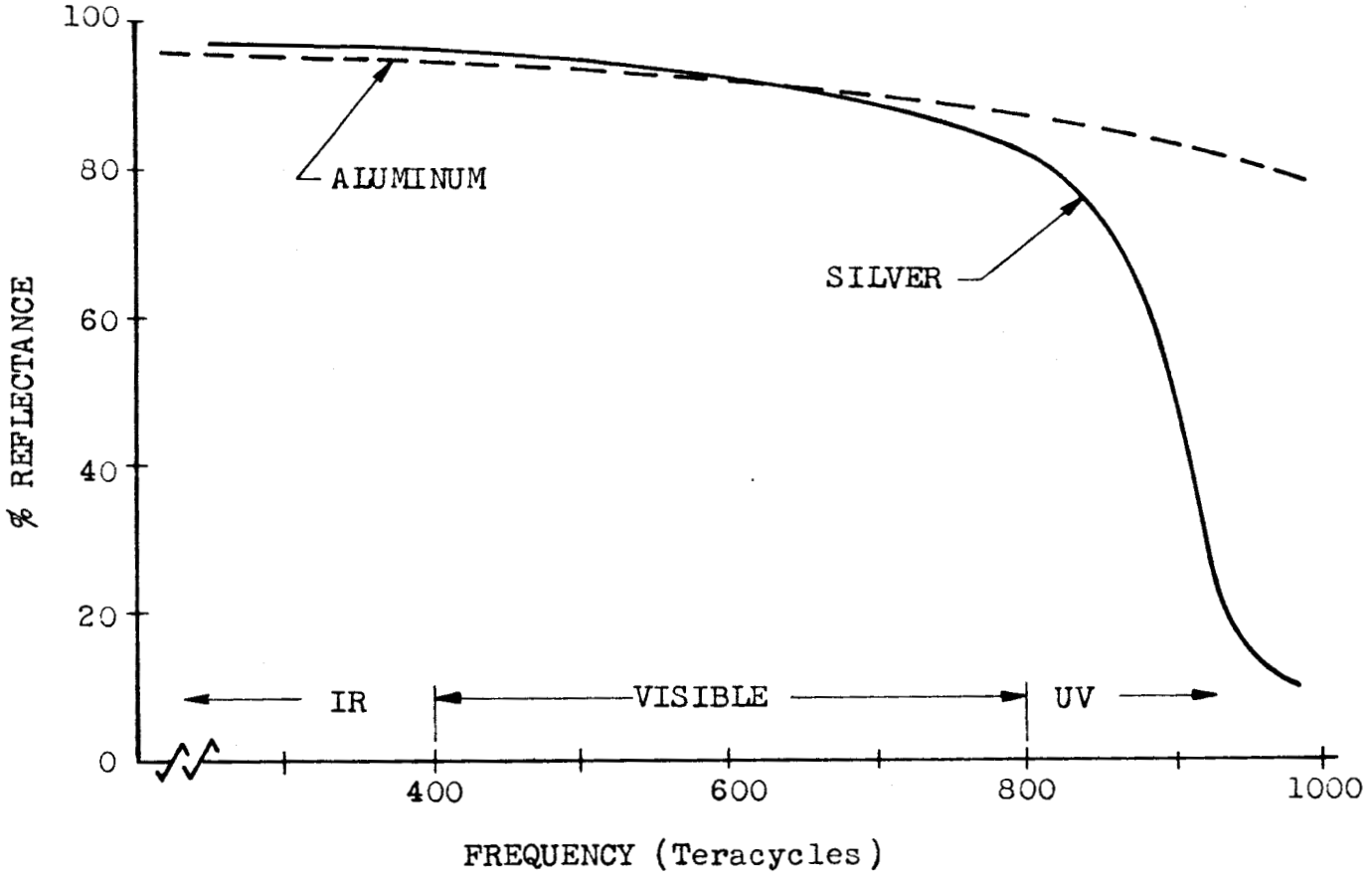

Fig. 16 - Reflectance of metals as a function of frequency.

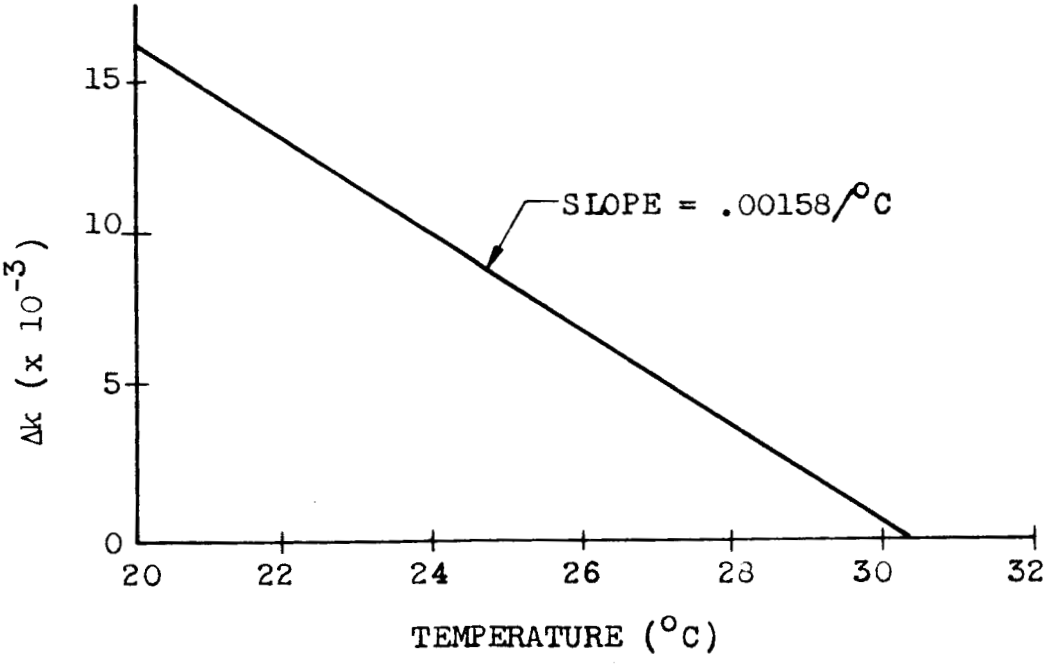

Fig. 17 - Temperature dependence of Δk for a chlorobenzene and glass waveguide.

vmg

$$\frac{k - 1}{k + 2} = \frac{4\pi}{3} N\alpha \,, \qquad (6)$$

where N is the density of molecules and α is the polarizability. For materials consisting of a variety of different molecules the $N\alpha$ product may be replaced by the summation of $N\alpha$ products over the different molecules. The polarizability, α, is a function of the quantum-mechanical state of the molecules (Ref. 10) and, is known to exhibit both a temperature and a frequency dependence.

The temperature variation of the dielectric constant arises from two separate effects. The predominant one for liquid dielectrics is the variation of density, N, with temperature and normally results in a decrease of dielectric constant with rising temperatures. The other factor is the temperature dependence of the polarizability. This is caused by thermal pumping of molecules into higher vibrational levels. The effect of the thermal pumping may be either to raise or lower the dielectric constant depending on the atomic structure of the material.

The dielectric constant of a solid is generally less temperature sensitive than that of a liquid. For typical glasses the dielectric constant changes by $0.00001/^{\circ}C$ while for typical liquids, it varies by $.001/^{\circ}C$. Therefore, in a completely solid waveguide the core and cladding have a similar temperature dependence so that Δk, the important parameter for waveguide propagation, will tend to remain constant even though the absolute value of the dielectric constant changes. The liquid-solid experimental waveguides, however, are very temperature sensitive because the dielectric constant of the liquid varies relative to that of the solid. The temperature dependence of Δk for a typical experimental waveguide is plotted in Fig. 17.

The frequency dependence of the dielectric constant is related to the molecular polarizability of the material. The polarizability exhibits various singularities as a result of molecular and atomic resonances. The frequency variation may be obtained from Eq. (6) by taking into account the frequency dependence of the polarizability which is given by;

$$\alpha = \frac{e^2}{M} \sum \frac{f_s}{(\omega_s^2 - \omega^2) + j\gamma_s \omega} \quad , \tag{7}$$

where f_s is the "oscillator strength" associated with each resonant frequency, ω_s, and γ_s is a damping term associated with each quantum transition. The summation is over all the resonant frequencies of the molecule. This theory has been developed from both classical and quantum mechanical viewpoints in Ref. 2 and will not be presented here. The dielectric constant as a function of frequency for a transparent dielectric is plotted over a large frequency band in Fig. 18, and the dielectric constant of borosilicate crown glass is shown in Fig. 19 for the visible portion of the spectrum. This material is typical of transparent optical materials in that dielectric constant increases with frequency.

The fabrication of a macroscopic optical waveguide is considered feasible for both experimental and prototype models. Experimental waveguides have already been demonstrated and the choice of waveguide materials may be based on published data and on simple laboratory measurements. Techniques for fabrication of more practical, prototype waveguides have been indicated. However, this application of these techniques is sufficiently different from conventional applications so that careful design and experimentation will be required for their development.

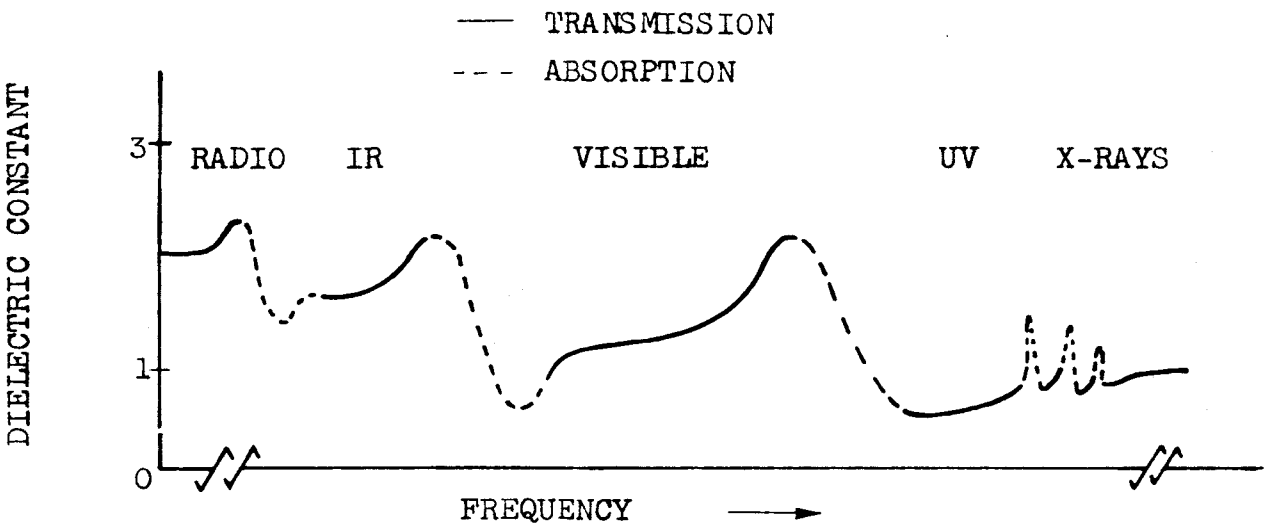

Fig. 18 - Typical variation of dielectric constant with frequency.

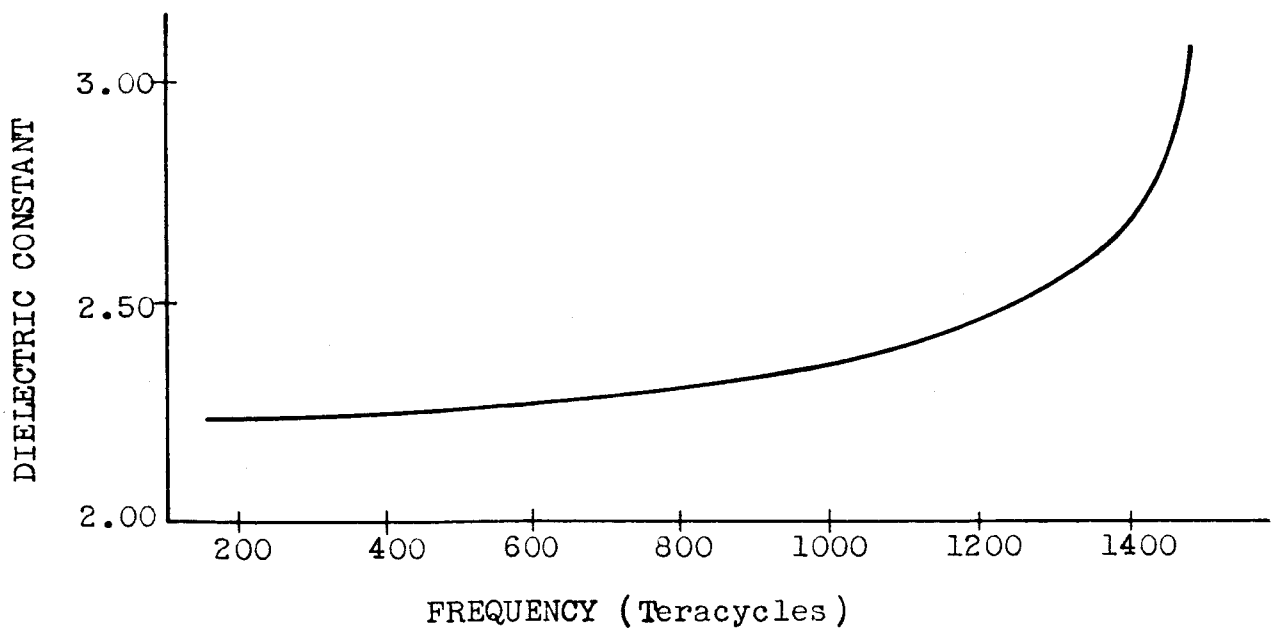

Fig. 19 - Dielectric constant versus frequency for borosilicate crown glass in the visible band.

vmg

V. Experimental Evaluation.

The objective of the experimental study is the verification of waveguide performance as predicted by the theoretical analysis. Positive verification will indicate that there is sufficient understanding of the waveguide propagation, and that adequate tolerances have been held on materials and configurations to justify the various assumptions of the analysis. The experimental program has included the observation of waveguide modes, the measurement of field patterns, and comparison of these characteristics with theoretical calculations, for several experimental waveguide configurations.

Three waveguide configurations have been investigated: (1) a liquid-core, solid-cladding dielectric-slab waveguide, (2) a solid-core, liquid-cladding dielectric-slab waveguide, and (3) a short-circuit-bisected dielectric-slab waveguide. These configurations are described below.

The experimental model of the first configuration, a liquid-core, solid-cladding dielectric-slab waveguide, was designed with the features shown in Fig. 20; a photograph of this waveguide is given in Fig. 15. The waveguide structure consists of two 77 mm plates of Schlieren quality borosilicate crown glass ($k = 2.2952$), suspended in chlorobenzene; the inside surfaces of the plates are optically flat. The glass plates serve as the waveguide cladding, and the chlorobenzene in the gap between the plates serves as the core.

The spacing between the plates is adjusted by means of a differential screw, shown in Fig. 20. One turn of the screw changes the spacing by ten microns. The spacing is observed through a 100X microscope, and measured with a calibrated reticle in the microscope eyepiece; the measurement accuracy is approximately $\pm$ 3 microns.

To provide a uniform waveguide, the plates have to be parallel. This is accomplished by directing a collimated laser beam through a side window on the waveguide tank, and observing the beams reflected from the surfaces of the glass plates with a telescope, as illustrated in Fig. 21. Each reflection appears as a point in the field of view of the telescope. When the points corresponding to reflections from the inner surfaces of the plates are superimposed, the plates are parallel. The adjustment is made with three differ-

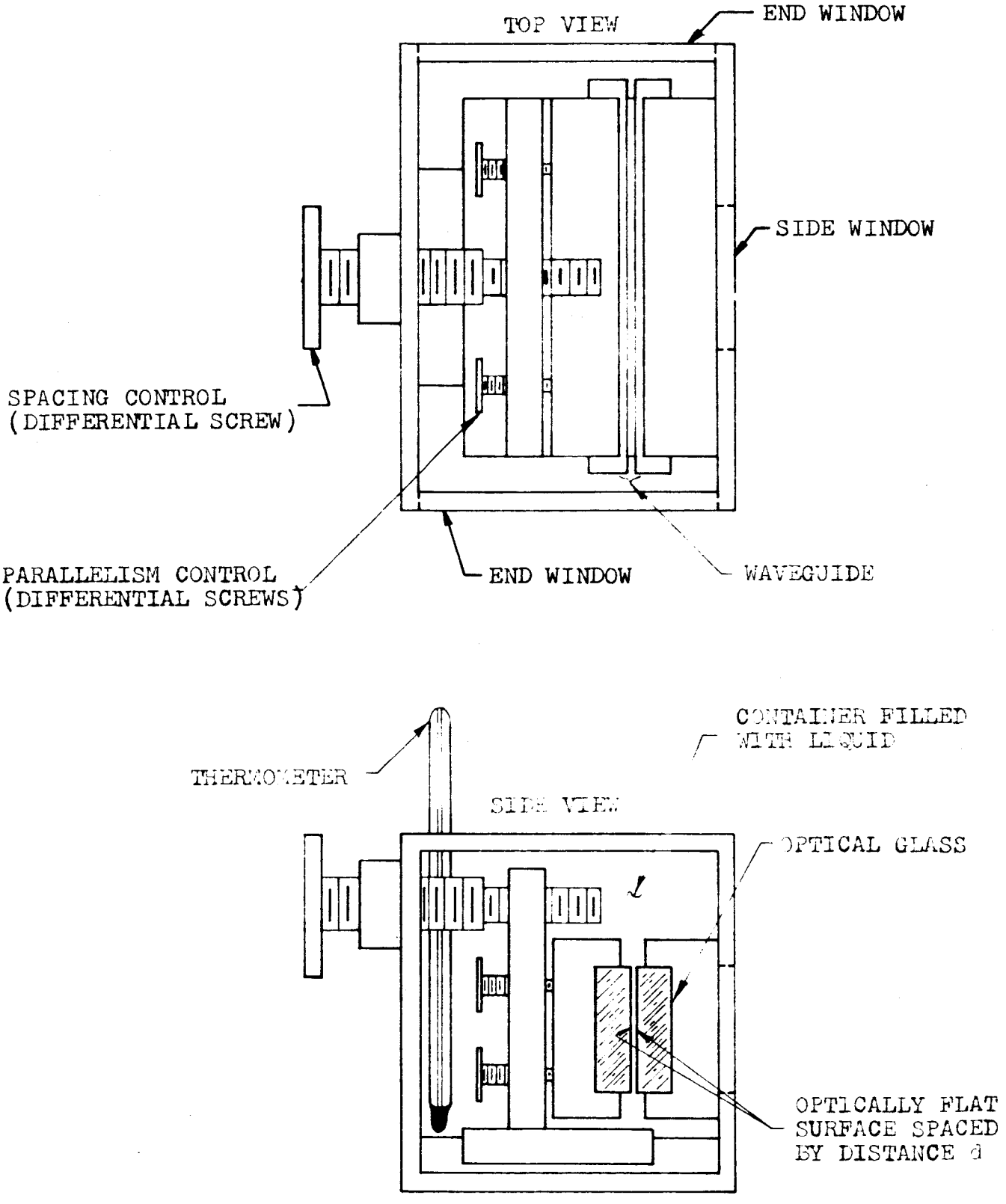

Fig. 20 - Experimental model of dielectric-slab waveguide.

wmg

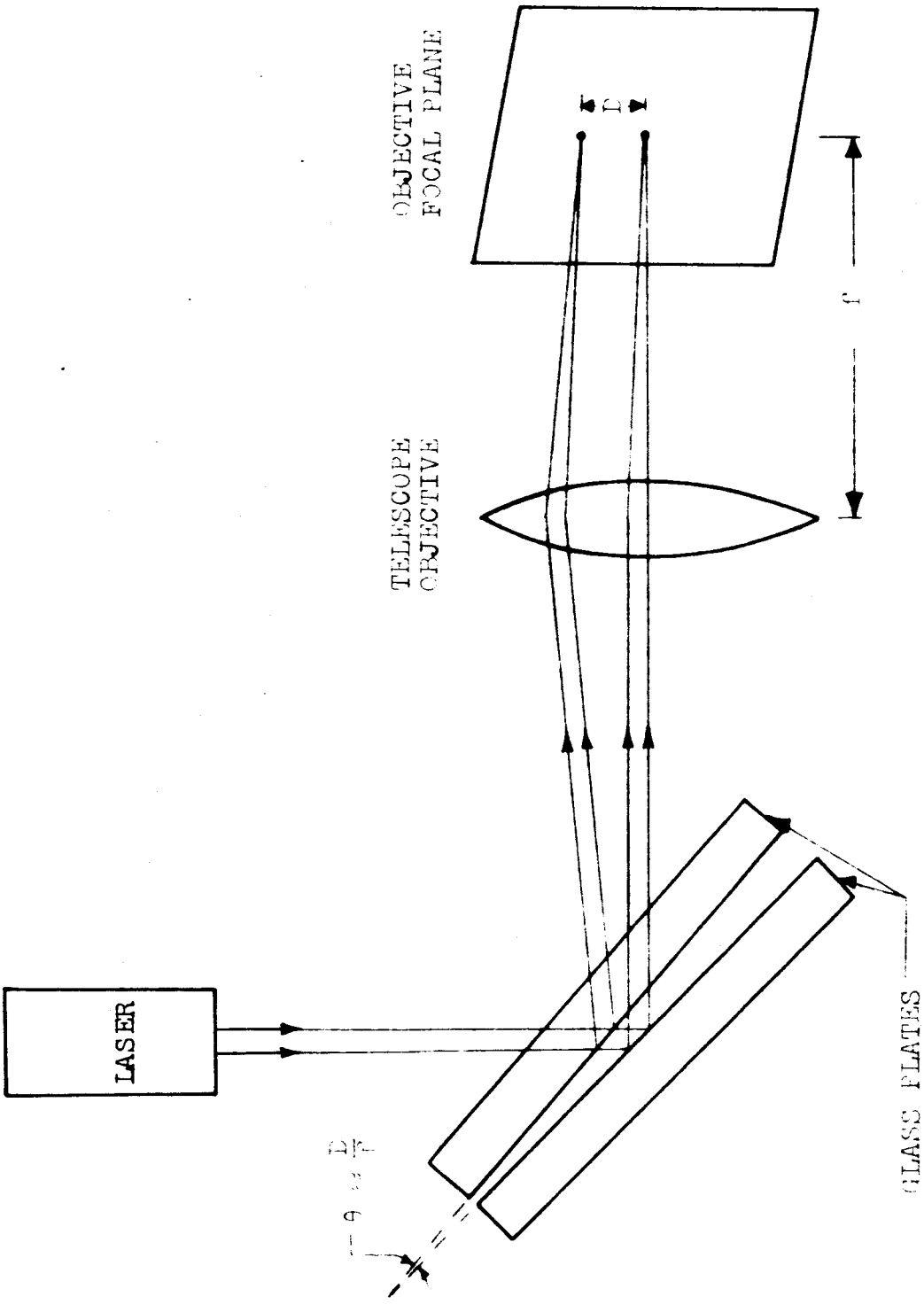

Fig. 21 - Technique for aligning glass plates.

ential screws, shown in Fig. 20. After adjustment, the plates are parallel to within 0.01 milliradian.

The experimental model of the second configuration, a short-circuit-bisected dielectric-slab waveguide, is similar in construction to the dielectric-slab waveguide described above; the only difference is that one of the glass plates has been replaced by an identical plate having a thin layer of aluminum deposited on the optically flat surface. The glass plate again serves as the cladding, and the chlorobenzene in the gap between the glass plate and the aluminized surface serves as the core. The adjustment of spacing and parallelism with this waveguide configuration are identical to those described above for the dielectric-slab waveguide.

The experimental model of the third configuration, a solid-core, liquid-cladding dielectric-slab waveguide, employs the same supporting structure as the waveguides described above. For the solid core guide, the two glass plates are removed and replaced by a thin (89 ± 3 microns) sheet of optical quality glass, 76 mm long, which serves as the waveguide core; the chlorobenzene in which it is suspended serves as the cladding.

In order to measure the number of modes and the field patterns, a test range has been implemented. This range comprises three basic systems: the source system, the waveguide system, and the detection system. A block diagram of the test range is given in Fig. 22; a photograph is shown in Fig. 23.

The source system, illustrated in Fig. 24, comprises a CW He-Ne gas laser having a collimated output at 0.6328 microns, provision for introducing a calibrated value of attenuation into the laser beam, and a lens for focusing the beam on the input aperture of the waveguide. The laser output is linearly polarized in the vertical plane; a half-wave plate may be placed in the beam to rotate the polarization to the horizontal plane when desired. A 1000 cps square-wave generator provides amplitude modulation of the laser.

The waveguide system, illustrated in Fig. 25, comprises the waveguide test fixture described previously, a thermostatically-controlled water-circulation system connected to the bottom of the waveguide tank, and provisions for adjusting the orientation of the

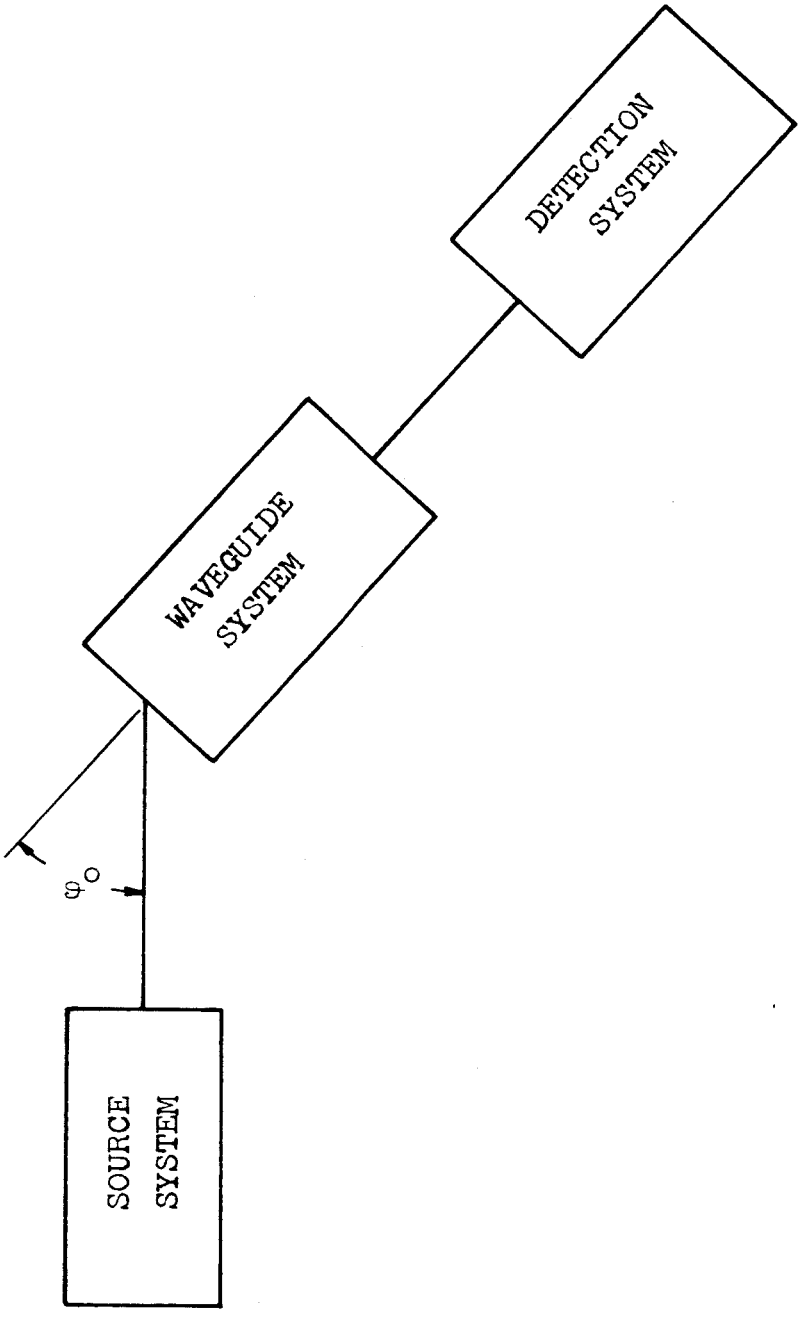

Fig. 22 - Block diagram of test range.

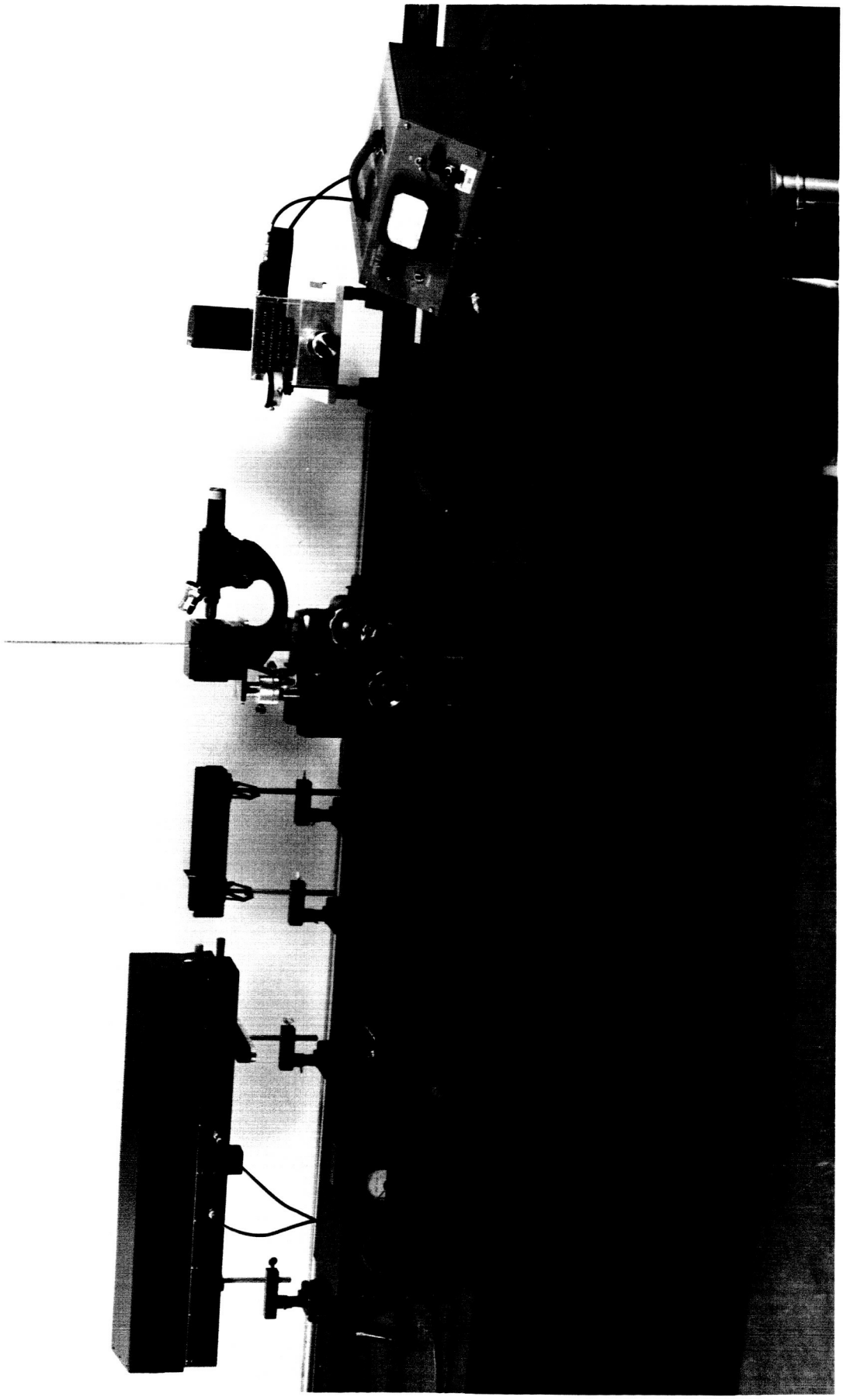

Fig. 23 - Photograph of test range for measurement of aperture distribution.

vmg

temperature, the difference in dielectric constant between the core and cladding is zero. The temperature was then decreased in discrete steps to increase the difference in dielectric constant. At each temperature level, the temperature was allowed to stabilize, and the excitation angle was varied. The highest propagating mode was noted, by counting the maximum number of lines observed in the core, and the corresponding mode number was indicated at a point on the mode chart (Fig. 27) corresponding to the measured values of waveguide spacing and difference in dielectric constant. It should be noted that the number of lines observed in the aperture for a given mode is one greater than the mode designation "m". For agreement between measurements and theory to be indicated, a highest mode number "m" would be observed for a point on the chart between the lines labeled "m" and "m+1". For small differences in dielectric constant, the data agrees with theory; as the difference increases, fewer modes were observed than predicted. However, within the precision and tolerances of the measurements and waveguide construction, it is considered that the waveguide modes observed are consistent with the theoretical analysis.

For the measurements of aperture field distributions, the waveguide width was first adjusted to be 75λ, the temperature of the waveguide was adjusted so that only the fundamental mode (TM-0, TE-0) was supported, and the excitation angle was adjusted for maximum output. A measured and theoretical pattern are shown in Fig. 28. The theoretical curve was obtained by noting the measured field amplitude at the edge of the core. This amplitude determines the values of the waveguide parameters "p" and "q", which in turn determine the theoretical field pattern (Appendix I). Good agreement between measurements and theory is obtained, indicating that waveguide performance is correctly explained by the analysis. A "noise" level at about -22 db is observed, and is caused by scattered light in the waveguide region. An additional aperture field pattern is presented in Fig. 29 for 50λ guide spacing. Although some asymmetry is present in this pattern, indicating that more than one mode is present, the general shape of the field is the same as that predicted by the analysis.

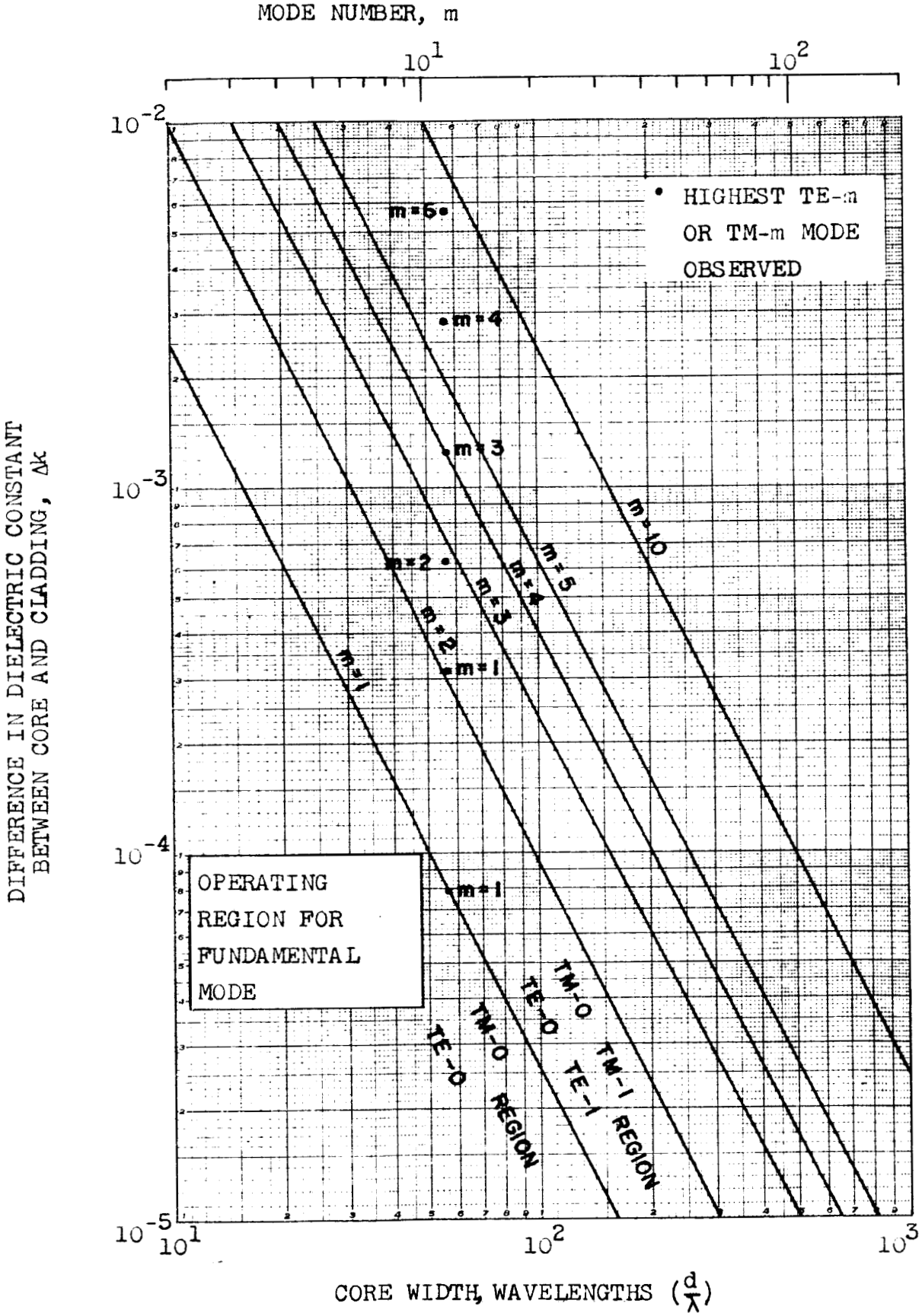

Fig. 27 - Mode chart, showing data for liquid-core, solid-cladding dielectric-slab waveguide.

vmg

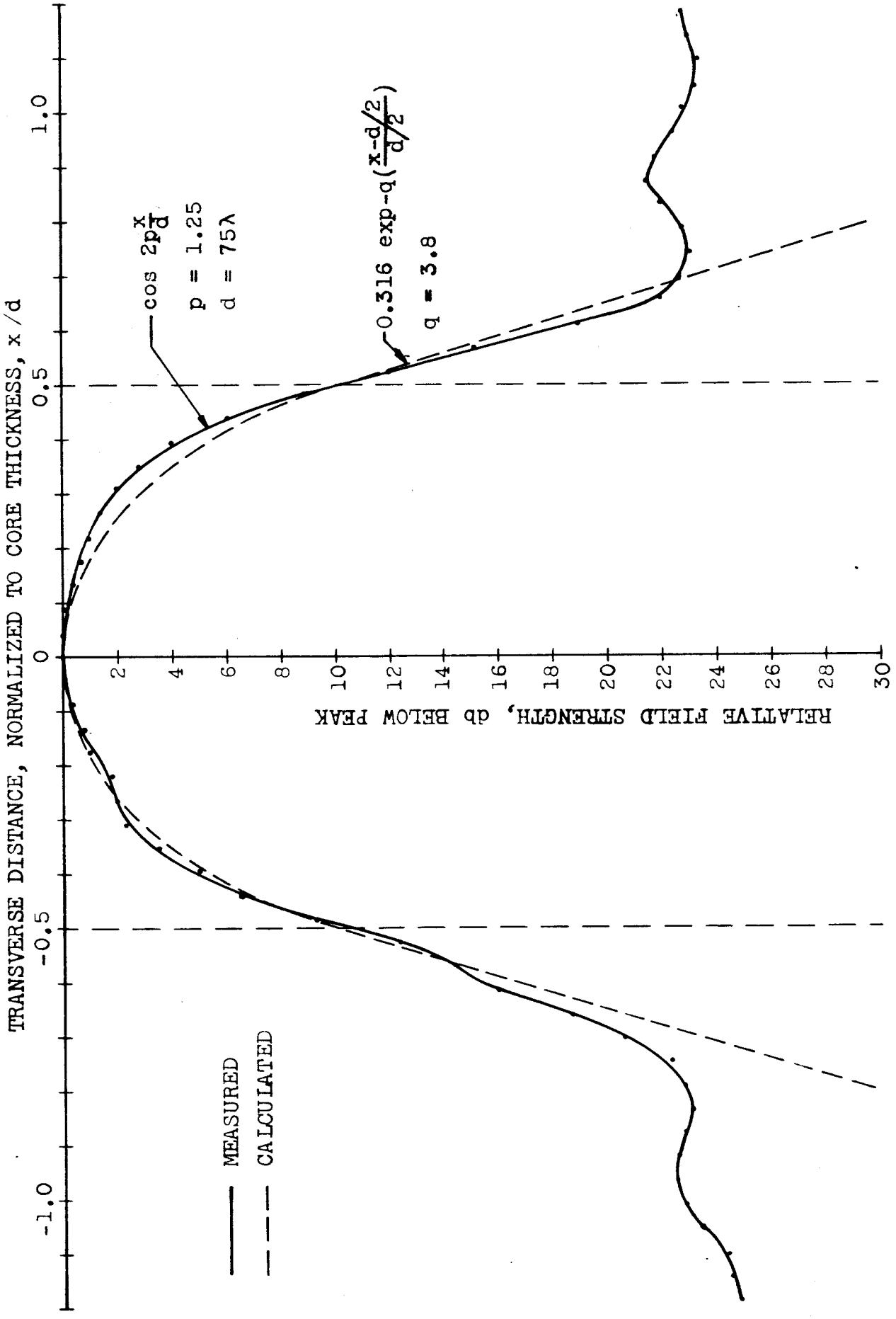

Fig. 28 - Aperture distribution, fundamental mode (TE-0) in liquid-core, solid-cladding dielectric-slab waveguide; 75λ spacing.

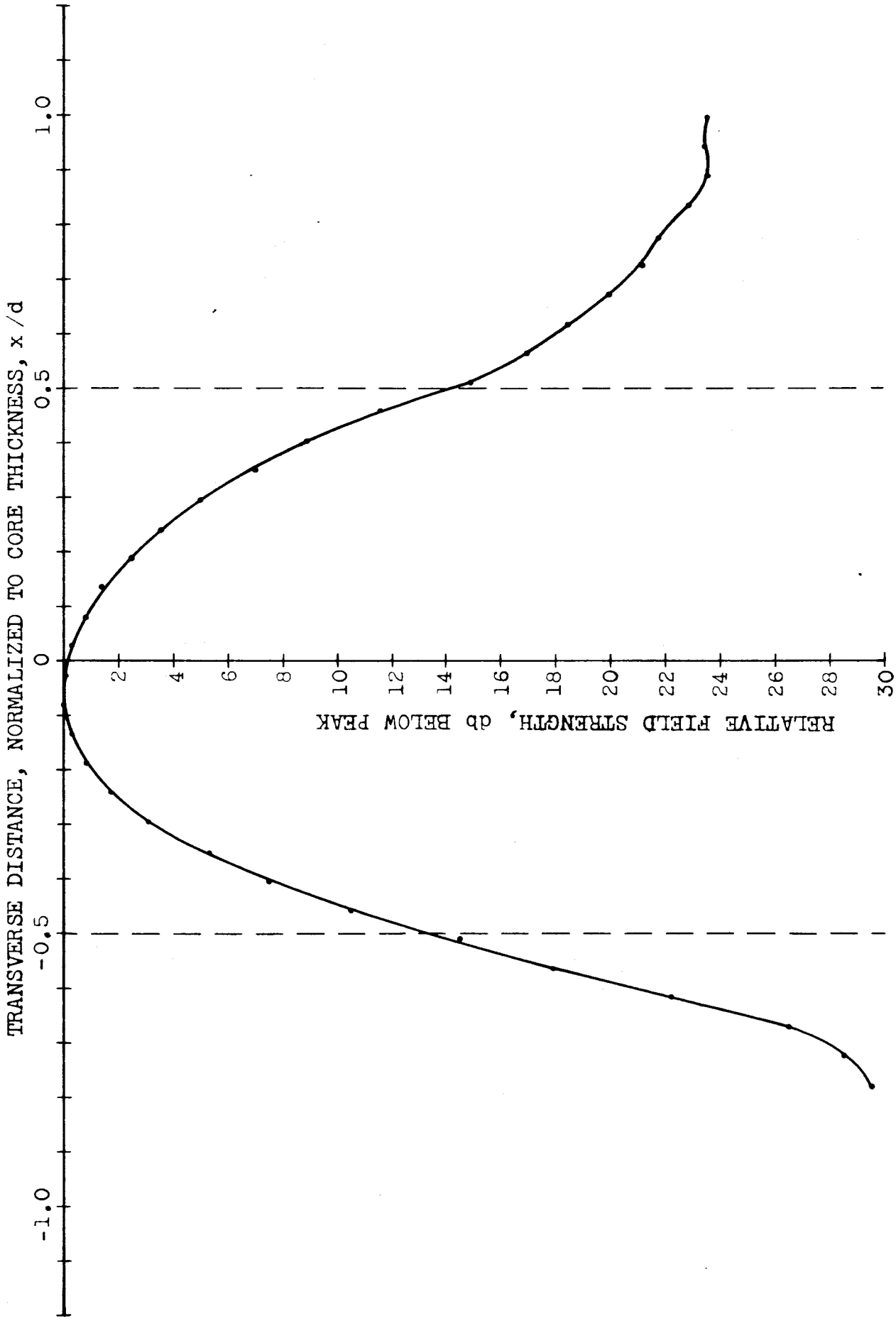

Fig. 29 - Aperture distribution, fundamental mode (TE-0) in liquid-core, solid-cladding dielectric-slab waveguide; 50λ spacing.

vmg

The temperature and excitation angle of the waveguide were subsequently adjusted to provide pure second-mode operation with a guide spacing of 31.6 microns (50λ). The measured pattern is plotted in Fig. 30. As in the fundamental-mode case, the pattern has the general characteristics predicted by the theory. However, the value at the center should be a null, but only a minimum was measured. This effect is caused by the photomultiplier, which has an aperture of some extent, and is an intensity-responding device. Therefore the depth of the minimum could not be measured accurately. The noise level was again approximately -22 db. The waveguide was then adjusted so that both the first and second modes propagated, in a guide of 83.0 micron (131λ) spacing, and the pattern was measured (Fig. 31). The general characteristics of the pattern again agree with the theory. The asymmetry in the pattern is a result of the vector addition of the fields of the two modes.

An attempt was made to observe and measure the radiation pattern for each of the three aperture distributions above. Because of spurious light transmission in the waveguide region, these observations were not possible at that time. However, observations were made for two cases of individual higher modes in a waveguide with 65.5 micron (103λ) spacing. When only the third mode was being propagated, the measured pattern angle was 0.03 radians, the same as the theoretical value. When the eighth mode was propagated, the measured pattern angle was 0.08 radians, also the theoretical value. These resilts further verify that the guide is operating according to the theoretical model assumed in the analysis.

2. Short-Circuit-Bisected Dielectric-Slab Waveguide.

This waveguide configuration was tested both for mode excitation and for field patterns as described above for the all-dielectric guide. The theoretical performance of this bisected waveguide, based on the assumption of a perfectly conducting metal wall, is similar in some respects to the dielectric guide, but differs in certain significant details. A metal wall forms a mirror and images some of the allowed modes, but does not permit others. To summarize briefly, every alternate TM mode is permitted starting

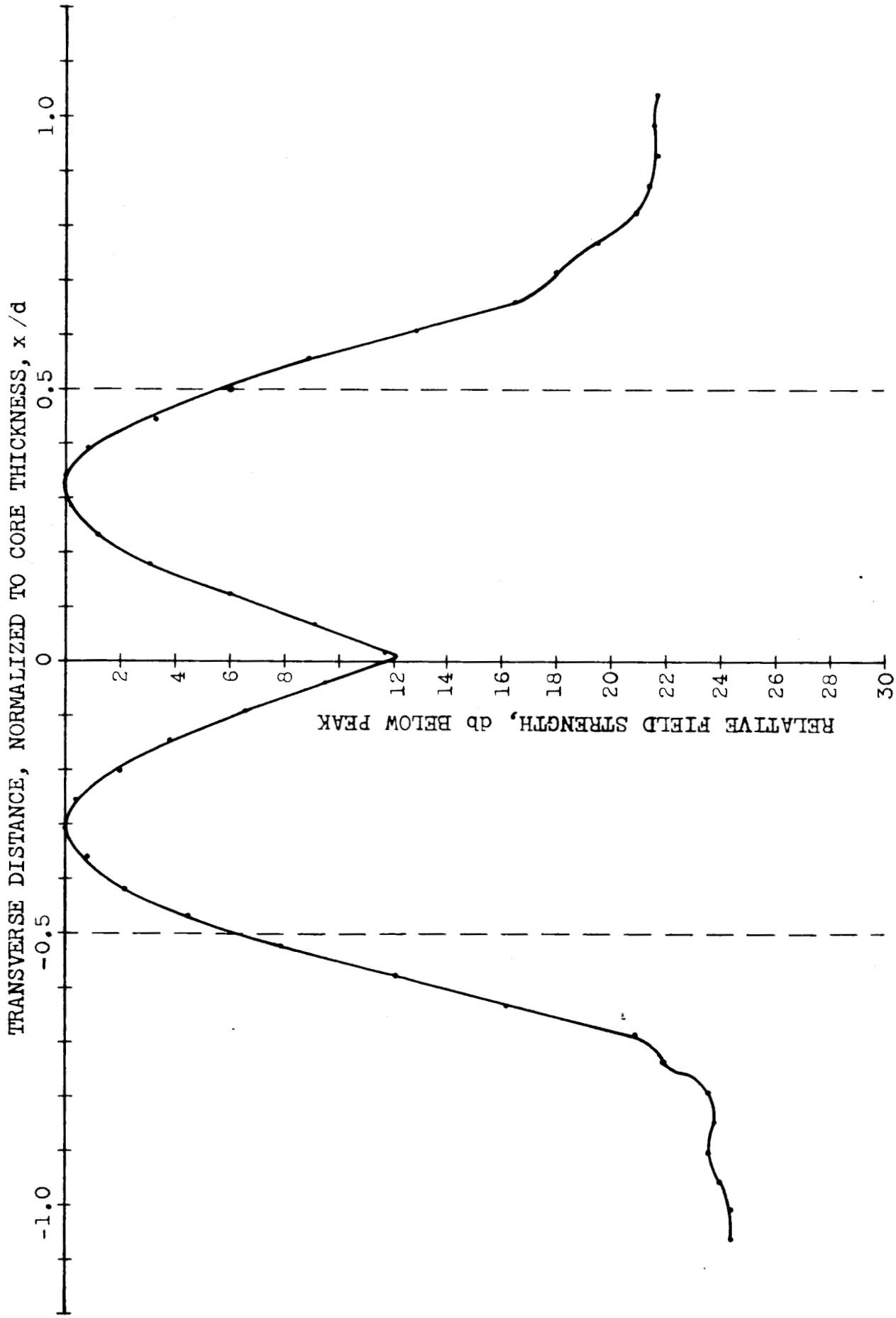

Fig. 30 - Aperture distribution, second mode (TE-1) in liquid-core, solid-cladding dielectric-slab waveguide; 50λ spacing.

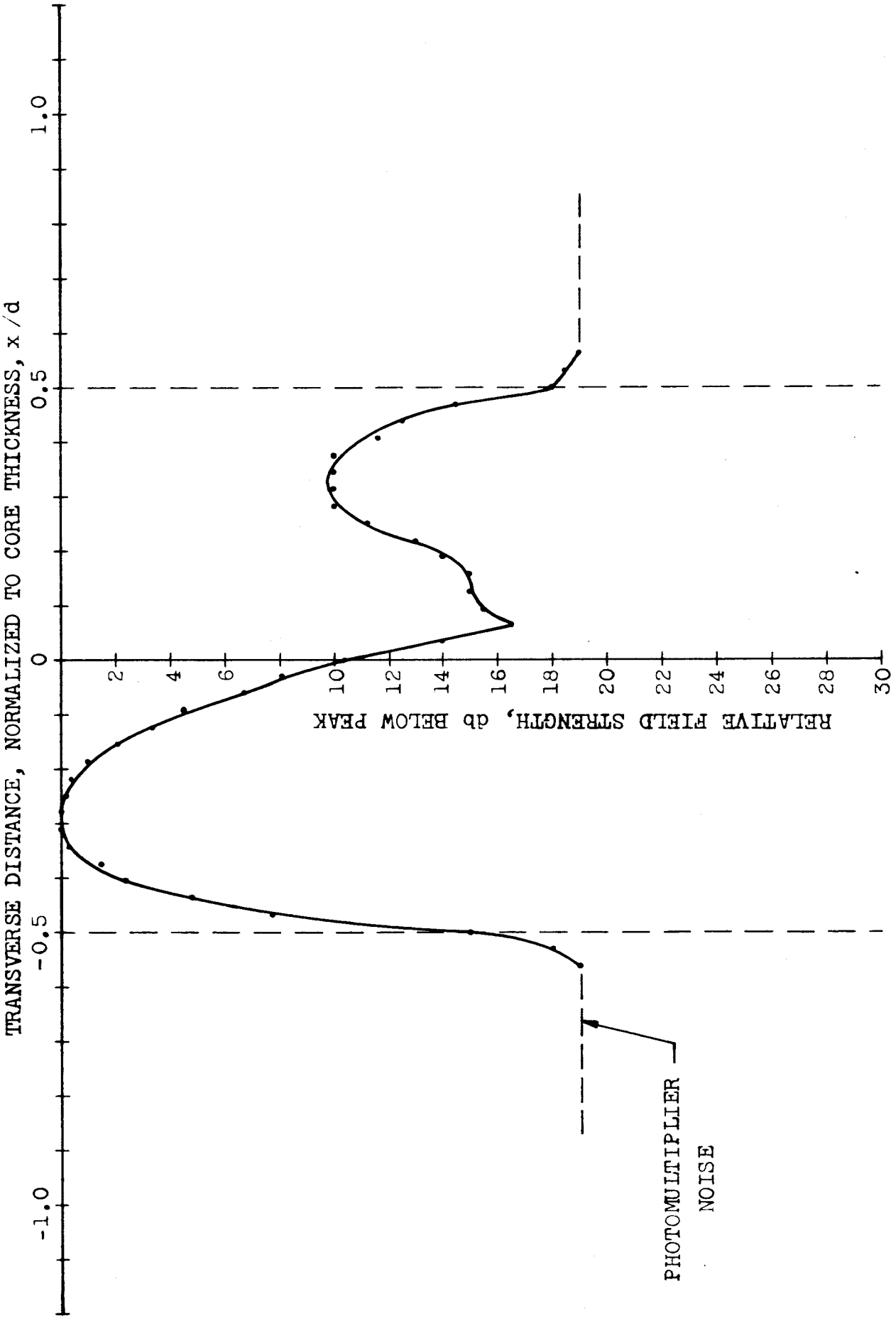

Fig. 31 - Aperture distribution, combination of first and second modes in liquid-core, solid-cladding dielectric-slab waveguide; 1.31λ spacing.

with the TM-0 mode (all modes with even mode number "m"). The lowest order TE mode is not allowed, but all modes with odd mode number "m" are permitted. The mode chart has the same cutoff lines as that for the dielectric guide, but represents only half of the modes. Each line represents the introduction of either a TE or TM mode, but not both simultaneously as for the unbisected guide. The width of the waveguide on the chart is equal to twice the actual separation between the metal surface and the boundary. The TM modes are characterized by maximum electric field amplitude on the metal wall and the TE modes by minimum electric field amplitude.

The first tests had as an objective the identification of the different shapes for the TM and TE modes, and the verification of the different cutoff conditions for the two types of modes. For these tests the waveguide temperature was adjusted so that only the fundamental mode was supported, and the excitation angle was adjusted for maximum output. The aperture distribution was then measured for both the TE and the TM modes by changing the incident polarization — Figs. 32 and 33 respectively. Both patterns are identical within experimental accuracy, indicating that contrary to theory the propagation characteristics are identical for the two modes.

The waveguide was then adjusted to provide second-mode operation, and the aperture distribution was measured for both the TE and the TM modes — Figs. 34 and 35 respectively. Both patterns are again, contrary to theory, identical within experimental accuracy. The fact that both peaks are not of equal amplitude indicates the presence of some fundamental mode, in addition to the desired second mode.

Additional tests were performed with greater difference in dielectric constant and additional TE and TM modes were observed. The main characteristic that became evident in all the above tests is that the TE and TM modes were identical in shape and cutoff characteristics, and therefore indicate a departure of measured performance from the theoretical model. A preliminary analysis suggests that this departure is caused by ohmic losses in the metal surface. These losses are great enough to change the phase of the reflection coefficient for parallel polarization (TM waves) from 0° to 180°, thus giving the TM waves the same propagation character-

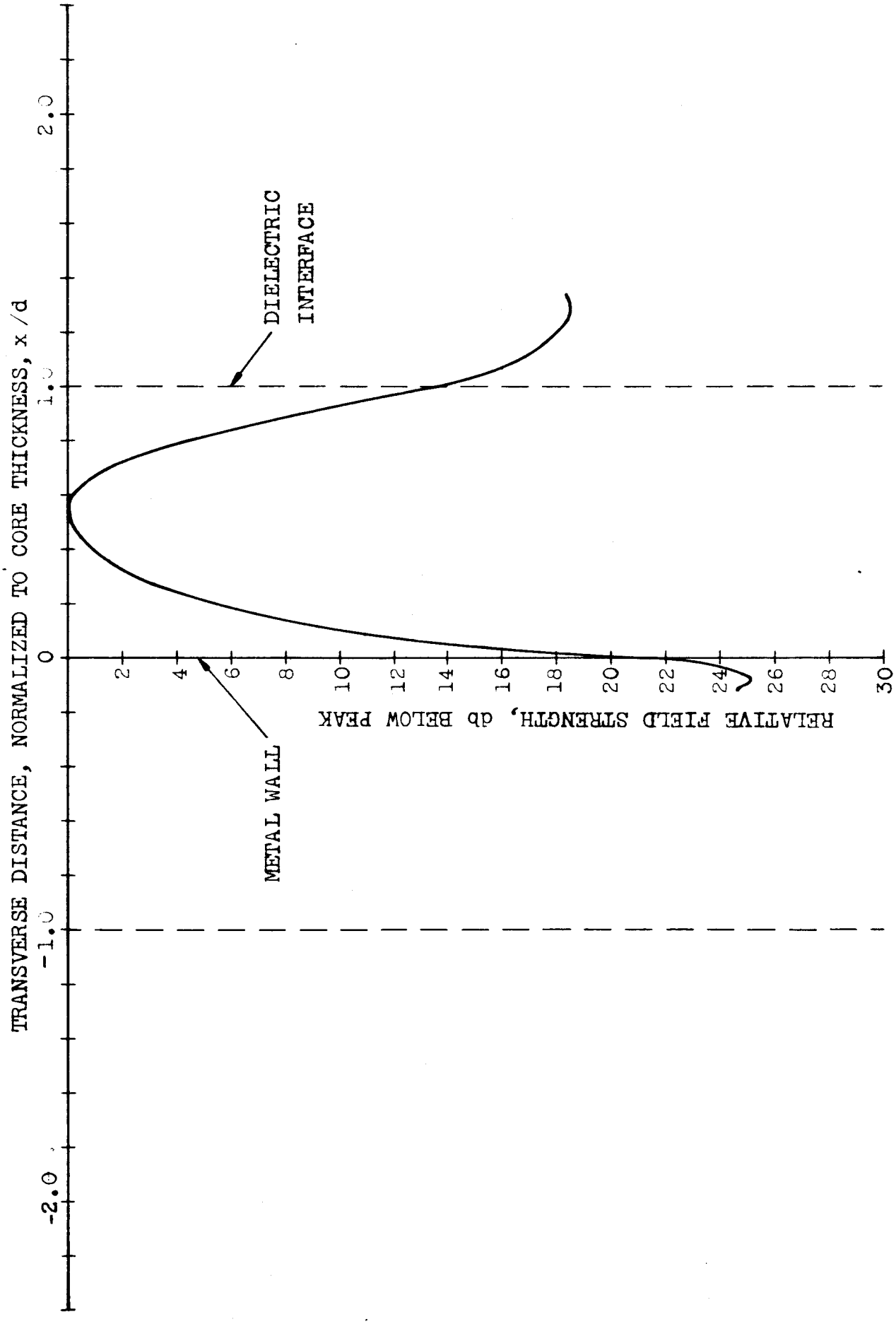

Fig. 32 - Aperture distribution, fundamental TE mode in bisected dielectric-slab waveguide; 50λ spacing.

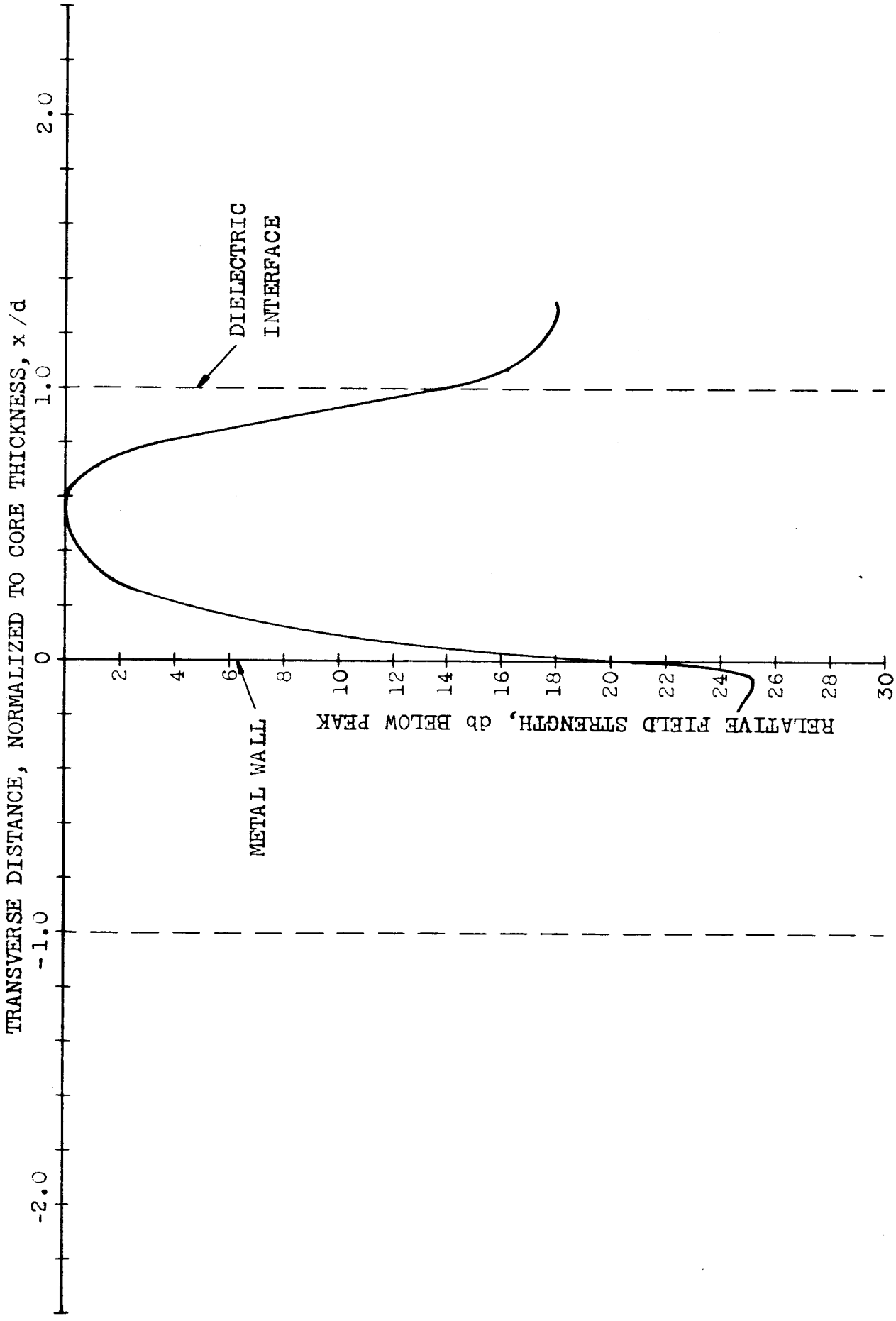

Fig. 33 - Aperture distribution, fundamental TM mode in bisected dielectric-slab waveguide; 5.0λ spacing.

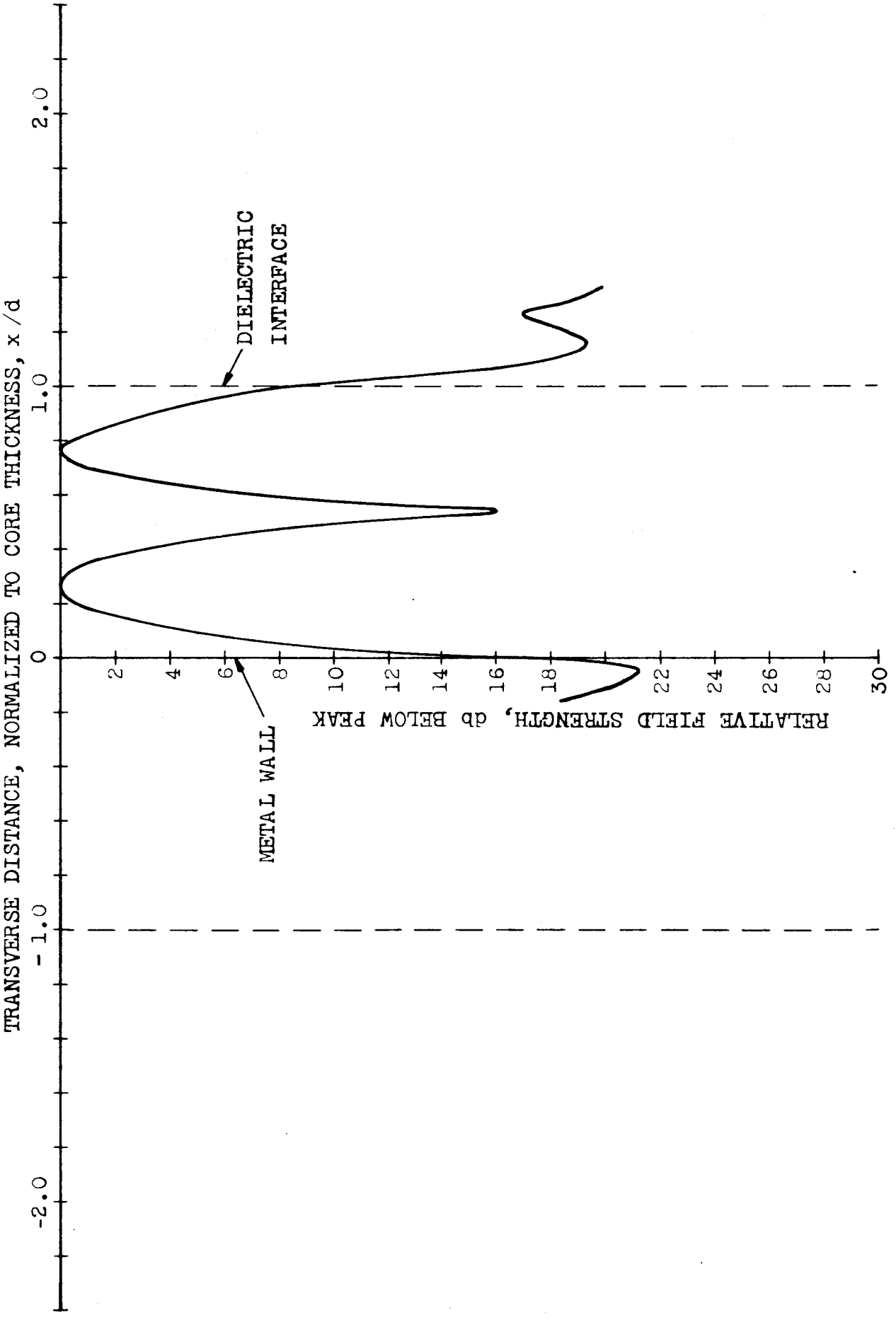

Fig. 34 - Aperture distribution, second TE mode in bisected dielectric-slab waveguide; 5.0λ spacing.

vmg

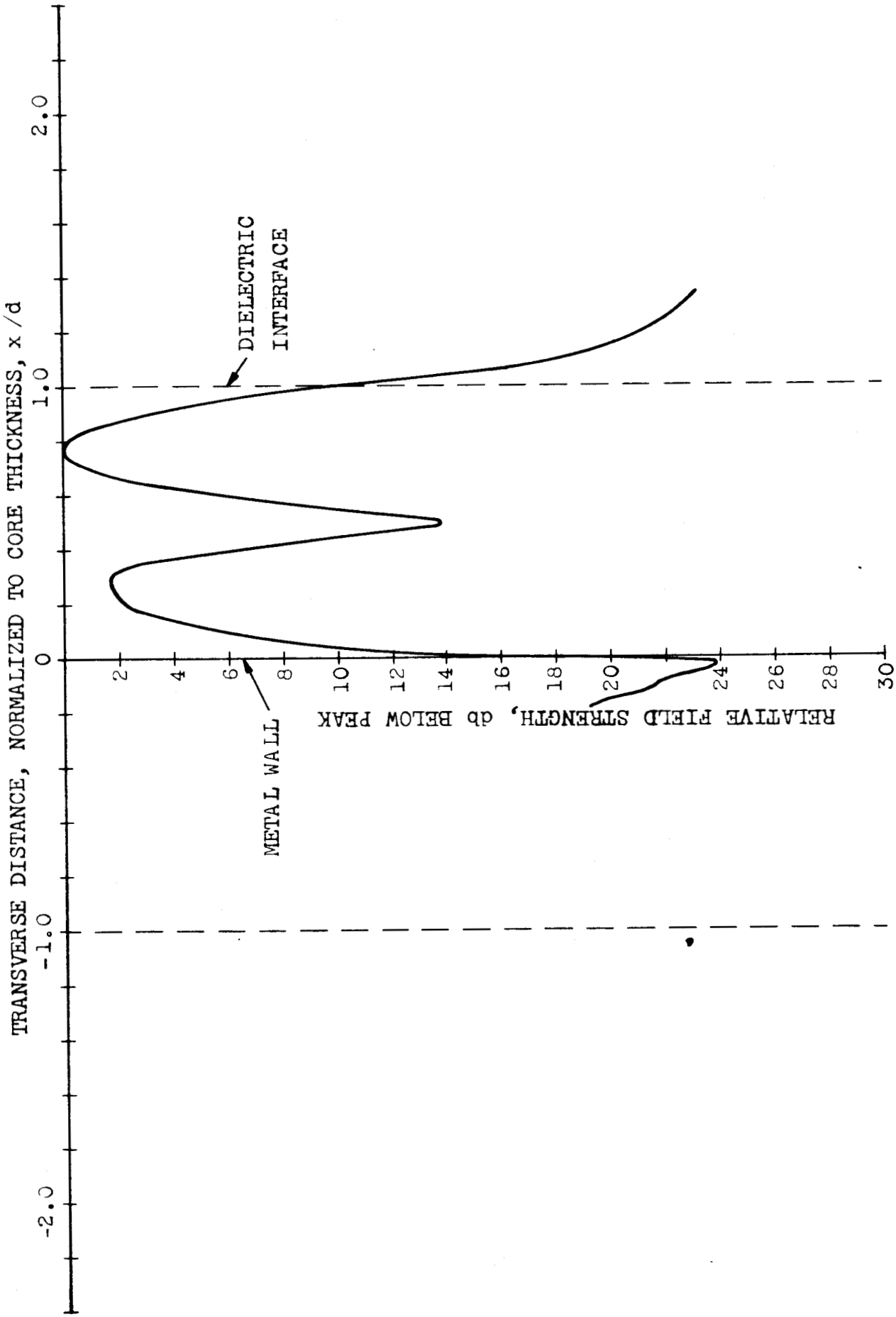

Fig. 35 - Aperture distribution, second TM mode in bisected dielectric-slab waveguide; 5.0λ spacing.

istics as TE waves. This type of behavior is often exhibited at microwaves and lower frequencies; one example is propagation of a ground wave over the earth, which has a finite conductivity. Since this behavior departs from the simple theoretical model assumed, further study is planned to understand the propagation characteristics for application to component design.

3. Solid-Core, Liquid-Cladding Dielectric-Slab Waveguide.

Preliminary observations were made with this configuration using a glass core of good, but not controlled, quality: no specifications were available on the dielectric constant, the homogeneity, or the flatness of the surfaces defining the core-cladding interfaces. The initial investigation revealed that individual higher modes could be propagated in this guide; they appeared to have the expected general characteristics.

An attempt to adjust this configuration for fundamental-mode operation, and measurement of the aperture distribution of the first several modes, is being deferred until thin glass sheets with controlled properties are received.

VI. Conclusions.

The properties of optical dielectric waveguide have been investigated for the case where the difference in the dielectric constants of the core and cladding materials is extremely small. In this waveguide, single-mode operation may be obtained with core dimensions of many wavelengths; thereby facilitating the fabrication of proposed microwave-type components.

The propagation characteristics of the waveguide have been analyzed using the conventional microwave technique of transverse resonance. From these computations the variations of the field intensities for the core and cladding regions have been obtained. This approach also yields the cut-off conditions which have been presented graphically in the form of mode charts. While the attenuation of this guide has been found to be high enough to preclude its use as a long distance transmission line, it is low enough so that lengths of a few centimeters, containing several microwave-type components, are considered feasible.

The problem of efficient waveguide excitation has also been studied theoretically; both for single-mode and multi-mode waveguides. It has been found that nearly all the power in an incident beam may be coupled into the lower waveguide modes by simple focusing techniques.

A number of techniques for waveguide fabrication have been considered. Throughout this work a distinction has been made between experimental waveguides, containing a liquid dielectric, and more practical, prototype waveguides which must be constructed entirely of solid dielectrics. Fabrication feasibility has been demonstrated by the operation of a laboratory model and sufficient design data has been obtained to permit the "electrical" design of a solid waveguide. However, the fabrication of an all solid waveguide is complicated by the tight tolerances required on the dielectric constants of the waveguide materials. Fabrication techniques are being studied and it is believed that the fabrication of a solid waveguide is feasible. Among the more promising techniques are (1) vacuum depositing of the cladding and (2) adjustment of the dielectric constant of a glass slab by physical or chemical changes.

vmg

The experimental program to date has consisted of a study of field distributions and cut-off conditions for several configurations. The cut-off conditions were determined by observing the highest order mode which could propagate for a given core thickness and difference in dielectric constant. The field plots were obtained in a manner similar to the measurement of microwave antenna patterns. The waveguide aperture distribution was transferred to a more accessible location by the focusing action of a microscope. Then this field distribution was scanned by a photomultiplier with a small sampling aperture. A servo system linked the scanning photomultiplier to a recorder which plotted the field distribution. The results of these measurements are in agreement with dielectric waveguide theory. An interesting result of these experiments was the realization that a short-circuit-bisected waveguide at optical frequencies does not exhibit the mode structure predicted by assuming a perfect conductor at the bisecting plane. It was found necessary to include the effect of the metallic losses to explain the observed modes.

In general, this study has demonstrated that single-mode waveguide with macroscopic dimensions at optical frequencies may be constructed and that the performance of this waveguide follows theoretical predictions.

vmg

VII. Acknowledgements.

The work described in this report has been performed during the period of 1964 JAN 28 to 1964 MAY 28 for the National Aeronautics and Space Administration under contract NASw 888. General direction has been provided by Roland Chase of NASA.

The work at Wheeler Laboratories has been performed by E. Ronald Schineller, Donald W. Wilmot, and Herman M. Heinemann under the direct supervision of Henry W. Redlien. Advice and general direction have been provided by Harold A. Wheeler and Frank H. Williams.

vmg

VIII. References.

(1) F. W. Fowle, "Smithsonian Physical Tables", 8 ed., Smithsonian Inst.; 1934.

(2) F. Seitz, "Modern Theory of Solids", 1 ed., McGraw-Hill; 1940.

(3) J. A. Ramsay, "Fourier Transforms in Aerial Theory", Marconi Review, no. 83, vol. 9 to no. 89, vol. 11; 1946-48.

(4) S. Silver, "Microwave Antenna Theory and Design", Rad. Lab. Series, vol. 12, McGraw-Hill; 1949.

(5) R. E. Beam et al, "Investigations of Multi-Mode Propagation in Waveguides and Microwave Optics", ASTIA No. ATI 94 929; Nov. 1950.

(6) A. A. Oliner, N. Marcuvitz, "Microwave Network Theory and Applications", MRI Report R-262-51, PIB-202, Polytechnic Inst. of Brooklyn; Sept. 1951.

(7) R. Meridith, "Radiation Patterns of Some Fourier Series Aperture Distributions", RRE Tech. Note 562, AD No. 90 782, Radar Research Est.; July 1955.

(8) D. D. King, S. P. Schlesinger, "Losses in Dielectric Image Lines", Trans. IRE, vol. MTT-5, p. 31; Jan. 1957.

(9) F. A. Jenkins, N. E. White, "Fundamentals of Optics", 3 ed. McGraw-Hill; 1957.

(10) E. Condon, H. Odishaw, "Handbook of Physics", 1 ed., McGraw-Hill; 1958.

(11) A. F. Harvey, "Periodic and Guiding Structures at Microwave Frequencies", Trans. IRE, vol. MTT-8, p. 30; Jan. 1960.

(12) A. F. Kay, "Near-Field Gain of Aperture Antennas", Trans. IRE, vol. AP-8, p. 586-593.

vmg

(13) N. S. Kapany, "Fiber Optics", Scientific Am., vol. 203, no. 5, p. 2-11; Nov. 1960.

(14) R. E. Collin, "Field Theory of Guided Waves", McGraw-Hill; 1960.

(15) E. Snitzer, "Cylindrical Dielectric Waveguide Modes", Jour. Opt. Soc. Am., vol. 51; May 1961.

(16) E. Snitzer, H. Osterberg, "Observed Dielectric Waveguide Modes in the Visible Spectrum", Jour. Opt. Soc. Am., vol. 51, p. 499; May 1961.

(17) E. Snitzer, "Optical Dielectric Waveguides", Advances in Quantum Electronics (J.R.Singer Ed.) Columbia Univ. Press, p. 348; 1961.

(18) H. Jasik, "Antenna Engineering Handbook", McGraw-Hill; 1961.

(19) R. W. Hermansen, "Mode Charts for Macroscopic Dielectric Waveguide at Optical Frequencies", WL Report 1137; July 1963.

(20) J. A. Ramsay, "Free Space Power Transmission", notes of talk presented to L.I. Chap. of PTGAP; Dec. 3, 1963.

(21) D. W. Wilmot, "Macroscopic Single-Mode Waveguide for the Construction of Optical Components", talk presented at 1964 PGMTT International Symposium, Long Island, N. Y.; May 20, 1964.

64 OC 12

NB 1425, 1426
1427, 1429, 1495
SNB 1427A, 1429A
1429B

E. Ronald Schmeller

Donald W. Wilmot

Herman M. Heinemann

myb

Appendix I. Analysis of Propagation in Dielectric Slab Waveguide by Transverse Resonance.

The propagation characteristics of dielectric slab waveguide can be determined either by a solution of the field equations in this structure with application of the appropriate boundary conditions, or by a transmission line type of analysis. This appendix indicates an analysis based on the transmission line technique of transverse resonance (Ref. 6). The basic approach is to consider the structure as a transmission line in the transverse direction and set up the conditions for resonance on this line. Certain resonant conditions in the transverse direction correspond to real propagating modes in the longitudinal direction of the guide.

The configuration of the dielectric slab waveguide is shown in Fig. 36(a). It consists of a dielectric slab of relative dielectric constant, k_1, and width, d, (waveguide core) bounded on both sides by a dielectric of relative dielectric constant, k_2 (cladding). The transverse waveguide equivalent circuit is shown in Fig. 36(b). It comprises a transmission line of length d, impedance Z_1, and propagation constant K_1 with semi-infinite lines of impedance Z_2 and propagation constant K_2 connected to each end as shown. A resonant condition in this waveguide exists if the impedance at some reference plane looking in one direction is equal to the negative of the impedance at this same plane looking in the other direction, that is,

$$\overleftarrow{Z}(x_1) + \overrightarrow{Z}(x_1) = 0 . \qquad (8)$$

This equation can be solved directly for the equivalent circuit indicated; however, because of the symmetry, the circuit can be bisected with an electric wall (short circuit) or a magnetic wall (open circuit) in order to simplify the analysis. The resulting equivalent circuits for these two cases are shown in Fig. 36(c) and (d). In order to find all the possible modes of propagation, both the short circuit and open circuit cases must be solved, and the analysis must be done for both transverse magnetic (TM) and transverse electric (TE) modes.

myb

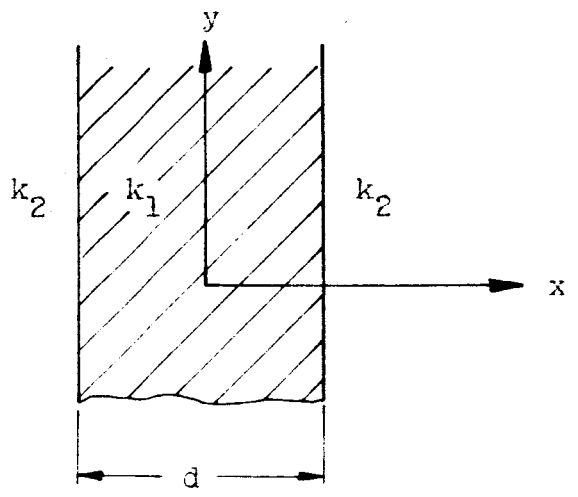

(a) Cross-section of dielectric slab waveguide.

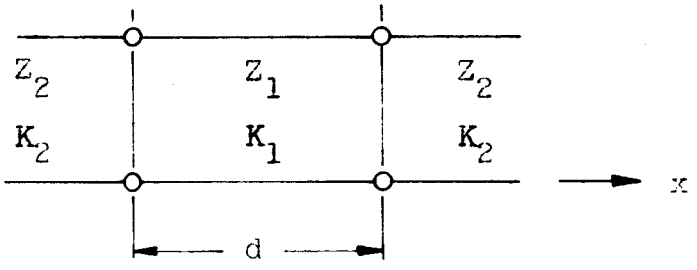

(b) Transverse equivalent circuit.

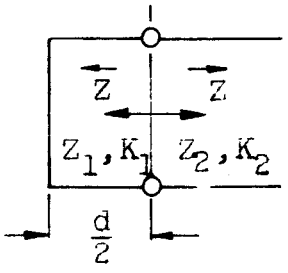

(c) Short circuit bisection.

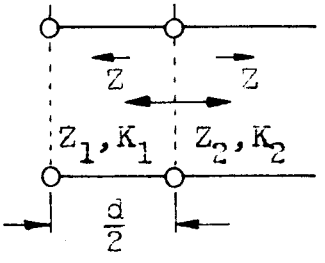

(d) Open circuit bisection.

Fig. 36 - Dielectric slab waveguide and equivalent circuits.

myb

The wave impedances in the core and cladding regions of the transverse equivalent waveguide are as follows. For the TM modes,

$$Z_1 = \frac{K_1}{\omega\epsilon_o k_1} ; \qquad Z_2 = \frac{K_2}{\omega\epsilon_o k_2} . \tag{9}$$

For the TE modes,

$$Z_1 = \frac{\omega\mu_o}{K_1} ; \qquad Z_2 = \frac{\omega\mu_o}{K_2} . \tag{10}$$

The method of analysis will be indicated for the TM modes with short circuit bisection. The other cases can be analyzed in an identical manner, and so only the results will be presented. The impedances looking to the right and left at the plane $x = d/2$ in Fig. 36(c) are substituted into equation (8);

$$jZ_1 \tan K_1 \frac{d}{2} + Z_2 = 0. \tag{11}$$

After substitution for Z_1 and Z_2, this equation can be written as,

$$K_1 \tan K_1 \frac{d}{2} = \frac{k_1}{k_2} |K_2| , \tag{12}$$

where K_2 has been replaced by $-j|K_2|$, since this propagation constant must be imaginary to obtain a solution.

For simplicity, the following parameters are defined, which include the propagation constants in the core and cladding, and the waveguide size:

$$K_1 \frac{d}{2} = p ; \tag{13}$$

$$|K_2| \frac{d}{2} = q . \tag{14}$$

Equation (12) above can now be rewritten in terms of the new parameters p and q as follows:

$$p \tan p = \frac{k_1}{k_2} q . \tag{15}$$

This is one of the basic characteristic equations for the dielectric slab waveguide. As derived above, it applies only to TM modes with a short circuit bisection. However, for the case of small Δk, the factor k_1/k_2 is very nearly equal to unity and can be neglected without appreciable error. This equation is then identical to the equation which would be obtained for TE modes with open circuit bisection. The corresponding equations for the TM open circuit and TE short circuit bisections are identical to equation (15) if the tangent function is replaced by the negative cotangent. Since the tangent and cotangent are related through a constant angle displacement in the argument, a single equation can be written to cover all cases:

$$p \tan \left(p - \frac{m\pi}{2}\right) = q \, . \tag{16}$$

The value of m in this equation designates the particular mode number, i.e., TM-m or TE-m mode. A value of m = 0 corresponds to the fundamental mode (TM-0 or TE-0).

The second characteristic equation is obtained from the following relationships between propagation constants:

$$K_1^2 = K_o^2 k_1 - K_z^2 \tag{17}$$

$$K_2^2 = K_o^2 k_2 - K_z^2 \, . \tag{18}$$

These equations can be combined and written in terms of the p and q parameters defined above to give the second characteristic equation:

$$p^2 + q^2 = K_o^2 \frac{d^2}{4} (k_1 - k_2). \tag{19}$$

Equations (16) and (19) are plotted on p vs. q coordinates in Fig. 37. These curves contain sufficient information to completely specify the propagation characteristics of a slab waveguide. The intersections of the curves given by equations (16) and (19) determine the values of p and q which simultaneously satisfy both equations, and hence satisfy the conditions for propagation. The conditions for mode cutoff can be readily obtained from these curves. For a guide to support

myb

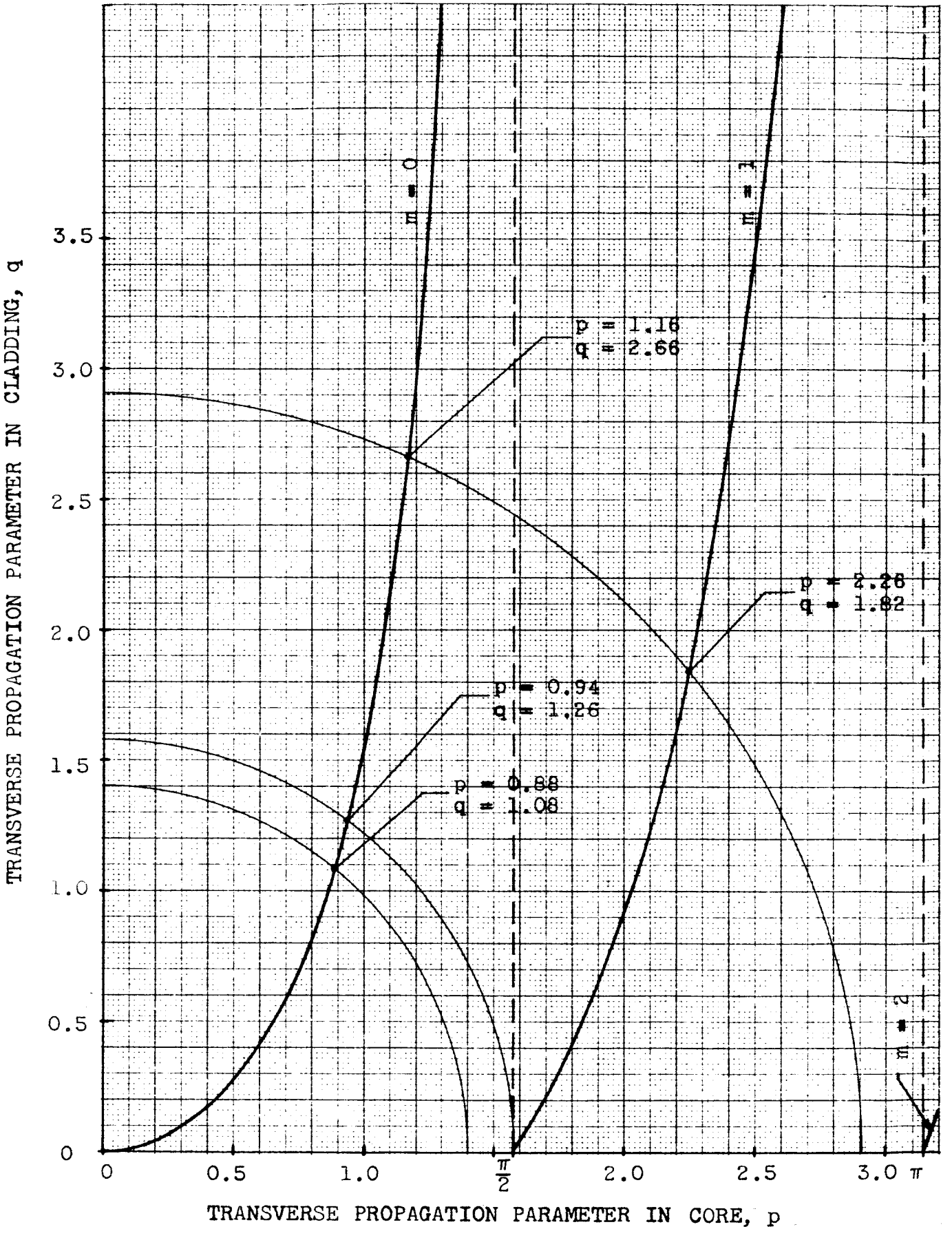

Fig. 37 - Characteristic p vs. q curves for dielectric slab waveguide.

myb

propagation in TM-m and TE-m modes and lower, the curves must intersect in at least m + 1 places (since m = 0 corresponds to the lowest modes). Conversely, if we wish to restrict propagation to only TM-m and TE-m modes and lower, the curves must intersect in only m + 1 places. This requires

$$K_o \frac{d}{2} (k_1 - k_2)^{1/2} < (m + 1) \frac{\pi}{2} , \tag{20}$$

or rewriting in terms of free space wavelength, λ,

$$\frac{d}{\lambda} \sqrt{\Delta k} < (m + 1) \frac{1}{2} . \tag{21}$$

For a single mode guide, therefore, the parameter $(d/\lambda)\sqrt{\Delta k}$ must be less than 1/2.

The field strengths in the waveguide core and cladding are functions of the transverse propagation constants in the respective regions. Therefore, the field distribution can be written in terms of p and q parameters. Expressions for the fields in the core and cladding regions for both TM and TE modes are given in Table III. These expressions are written in terms of the p and q parameters, a wave impedance which depends on the particular field component and a factor, A. A contains a factor A_m, related to the absolute fields in the guide, and the waveguide propagation factor, $\exp - K_z z \exp j\omega t$, which is the same for all the fields. All of these factors are essentially independent of the waveguide parameters for the case of small Δk, except for the functions of p and q. Therefore, these parameters determine the field distributions almost exclusively. A plot of the transverse fields of the two lowest order modes in slab waveguide is shown in Section III, for several different operating conditions. The values of p and q at these operating points are indicated on the curves of Fig. 37.

The dispersion properties of the waveguide are the variations of propagation constant with frequency and waveguide dimensions. The variation of guide wavelength with free space wavelength is a common way of expressing the dispersion. Guide wavelength is related to the propagation constants as follows:

TM-MODES	TE-MODES
FIELDS IN CORE	
$H_y = A \cos \left(\frac{2px}{d} - \frac{m\pi}{2}\right)$	$E_y = A' \cos \left(\frac{2px}{d} - \frac{m\pi}{2}\right)$
$E_x = -A\, Z_{z_1} \cos \left(\frac{2px}{d} - \frac{m\pi}{2}\right)$	$H_x = A'\, Z_{z_1} \cos \left(\frac{2px}{d} - \frac{m\pi}{2}\right)$
$E_z = -jA\, Z_1 \sin \left(\frac{2px}{d} - \frac{m\pi}{2}\right)$	$H_z = -jA'\, Z_1 \sin \left(\frac{2px}{d} - \frac{m\pi}{2}\right)$
FIELDS IN CLADDING	
$H_y = A \cos b_m \exp - q\left(\frac{x-d/2}{d/2}\right)$	$E_y = A' \cos b_m \exp - q\left(\frac{x-d/2}{d/2}\right)$
$E_x = -A\, Z_{z_2} \cos b_m \exp - q\left(\frac{x-d/2}{d/2}\right)$	$H_x = A'\, Z_{z_2} \cos b_m \exp - q\left(\frac{x-d/2}{d/2}\right)$
$E_z = -jA\, Z_2 \sin b_m \exp - q\left(\frac{x-d/2}{d/2}\right)$	$H_z = -jA'\, Z_2 \cos b_m \exp - q\left(\frac{x-d/2}{d/2}\right)$

$$A = A_m \exp - j K_z z \exp j\omega t$$

$$A' = A'_m \exp - j K_z z \exp j\omega t$$

$$b_m = p - \frac{m\pi}{2}$$

Table III - Expressions for field components in dielectric slab waveguide.

myb

$$\frac{\lambda}{\lambda_g} = \frac{K_z}{K_o} \quad . \tag{22}$$

The factor K_z/K_o can be written in terms of the p and q parameters:

$$\frac{\lambda}{\lambda_g} = \left[\frac{k_2 p^2 + k_1 q^2}{p^2 + q^2}\right]^{1/2} \quad . \tag{23}$$

This expression can be written in many forms to find the variation with particular waveguide parameters. The variation of guide wavelength (λ/λ_g) is plotted as a function of the guide width in wavelengths (d/λ) in Section III of this report.

myb